Apico-basal elongation requires a drebrin-E–EB3 complex in columnar human epithelial cells

Elsa Bazellières[1,2], Dominique Massey-Harroche[1,2], Magali Barthélémy-Requin[1,2], Fabrice Richard[1,2], Jean-Pierre Arsanto[1,2] and André Le Bivic[1,2,*]

[1]CNRS, UMR 6216, Developmental Biology Institute of Marseille Luminy (IBDML), case 907, 13288 Marseille, CEDEX 09, France
[2]Université de la Méditerranée, Developmental Biology Institute of Marseille Luminy (IBDML), case 907, 13288 Marseille, CEDEX 09, France
*Author for correspondence (andre.le-bivic@univmed.fr)

Accepted 15 September 2011
Journal of Cell Science 125, 919–931

doi: 10.1242/jcs.092676

Summary

Although columnar epithelial cells are known to acquire an elongated shape, the mechanisms involved in this morphological feature have not yet been completely elucidated. Using columnar human intestinal Caco2 cells, it was established here that the levels of drebrin E, an actin-binding protein, increase in the terminal web both in vitro and in vivo during the formation of the apical domain. Drebrin E depletion was found to impair cell compaction and elongation processes in the monolayer without affecting cell polarity or the formation of tight junctions. Decreasing the drebrin E levels disrupted the normal subapical F-actin–myosin-IIB–βII-spectrin network and the apical accumulation of EB3, a microtubule-plus-end-binding protein. Decreasing the EB3 levels resulted in a similar elongation phenotype to that resulting from depletion of drebrin E, without affecting cell compaction processes or the pattern of distribution of F-actin–myosin-IIB. In addition, EB3, myosin IIB and βII spectrin were found to form a drebrin-E-dependent complex. Taken together, these data suggest that this complex connects the F-actin and microtubule networks apically during epithelial cell morphogenesis, while drebrin E also contributes to stabilizing the actin-based terminal web.

Key words: Apical differentiation, Actin network, Terminal web, Epithelial morphogenesis, EB3 microtubule binding protein

Introduction

The complex process of epithelial morphogenesis results in the unique pattern of protein distribution typical of epithelial cells, which enables them to perform their various physiological functions (reviewed by Rodriguez-Boulan and Nelson, 1989). Intestinal epithelial cells differentiate during their migration along the crypt–villus axis and acquire an elongated shape and an apical brush border consisting of microvilli anchored in a dense actin-based network called the terminal web (Drenckhahn and Dermietzel, 1988; Fath et al., 1990; Gordon and Hermiston, 1994; Massey-Harroche, 2000). Actin rearrangements must occur in order to generate the typical narrow, elongated shape of the columnar epithelial cells and the dense meshwork consisting of the apical terminal web and bundles of microvilli (Bretscher and Weber, 1980; Ezzell et al., 1989; Fath et al., 1990; Lin et al., 1994). The actin-binding proteins required to obtain this highly specialized apical morphology and a properly organized terminal web include villin, fimbrin, spectrin, myosin II and ankyrin (Heintzelman et al., 1994; Pearl et al., 1984; Peterson and Mooseker, 1993). Proteins belonging to the ezrin–radixin–moesin (ERM) family are also involved in regulating the formation of the subapical cytoskeleton (Berryman et al., 1993; Saotome et al., 2004), and it seems very likely that apico–basal elongation and compaction processes might require many other actin-interacting proteins.

Among these proteins, the developmentally regulated brain protein known as drebrin is an F-actin-binding protein that was first described in neuronal tissues, where it is involved in morphogenetic events (Shirao and Obata, 1985). Drebrin A and E isoforms have been found to control the morphology and axonal growth, respectively, of hippocampal neurons in vitro. Drebrin E is involved in particular in controlling axonal growth by regulating the process of F-actin accumulation at the growing tip of the axon, along with EB family member 3 (EB3, also known as microtubule end-binding protein 3) (Geraldo et al., 2008). Overexpression of drebrin E results in axonal lengthening, which can be reversed by inhibiting myosin II activity: this suggests that these three proteins might interact (Mizui et al., 2009). By contrast, the targeting of NMDA receptors to the appropriate synapses requires the presence of drebrin A in these hippocampal neurons (Takahashi et al., 2003).

In epithelial cells, where only drebrin E is expressed, this protein has been found to connect gap junctions to the actin cytoskeleton (Butkevich et al., 2004). Interestingly, it has also been established that drebrin E accumulates in the apical region of epithelial cells in both the stomach and kidney, two epithelia with highly differentiated surfaces (Keon et al., 2000). This pattern of distribution prompted us to investigate whether drebrin E might be involved in the development of the apical actin cytoskeleton in human epithelial cells during morphogenesis and how drebrin E might ultimately contribute to regulating the shape of these cells.

Caco2 cells were used here as a model for the highly polarized and differentiated intestinal cells (Peterson et al., 1993; Peterson and Mooseker, 1993; Saaf et al., 2007). When these cells are confluent, their apico–basal axis is lengthened, and the apical region is concomitantly constricted. During this process, drebrin E accumulates in the terminal web, along with F-actin. Drebrin E depletion resulted in larger and flatter cells that lacked a properly organized brush border and terminal web, thus perturbing

Journal of Cell Science

terminal differentiation. Interestingly, the depletion of EB3 (a protein associated with the plus-ends of microtubules) gave rise to flatter, but not larger, cells, mimicking the drebrin E elongation phenotype. No obvious effects on apico–basal polarity or tight junction morphology or function were observed in either case. Drebrin E expression was found to be a requisite for the appropriate subapical F-actin, βII spectrin, myosin IIB and EB3 accumulation, and it was observed that EB3, βII spectrin and myosin IIB co-immunoprecipitate only when drebrin E is expressed. Taken together, these data therefore suggest that drebrin E and EB3 are essential for the typical shape of columnar epithelial cells to be generated by the coupling between F-actin and microtubules.

Results

Drebrin E accumulates in the subapical region of Caco2/TC7 cells and human enterocytes

To determine how drebrin E contributes to epithelial cell morphogenesis, the subcellular distribution of drebrin E was first examined in human small intestine and colonic Caco2/TC7 cells, which are highly polarized and show a typical enterocytic brush border after differentiating (Chantret et al., 1994). Drebrin E was found to form puncta along the lateral membrane and a dense network across the entire subapical region in both Caco2/TC7 cells and human enterocytes (Fig. 1A; supplementary material Fig. S1B). This accumulation of drebrin E in the subapical region besides its lateral presence indicates that it might be involved in regulating the organization of actin at the apical pole of epithelial cells.

Drebrin E depletion induces a dramatic change in Caco2/TC7 cell morphology without affecting cell polarity, tight junction formation, function or maintenance

In order to establish whether drebrin E contributes to epithelial morphogenesis, siRNA methods were used to reduce the drebrin E levels in Caco2/TC7 cells. Quantitative western blot analysis of drebrin E showed that the total level of expression decreased by 82%±10 (s.d.) on day 3 and by 75%±14 (s.d.) on day 5 in knockdown (KD) cells in comparison with control (CT) cells (supplementary material Fig. S2A). Despite considerable efforts, we were unable to generate stable Caco2/TC7 cell lines devoid of drebrin E using shRNAs, which indicates that drebrin E might contribute importantly to cell proliferation and/or survival. All the drebrin E depletion experiments described below were therefore based on the use of transient transfection methods. It must be noted that, at day 5 of confluence, Caco2/TC7 cells have not yet reached their full terminal differentiation but already have all the key features of this terminal differentiation, including cell polarity, functional tight junctions, a terminal web and some brush border (Chantret et al., 1994).

To test whether drebrin E depletion affects the appropriate formation of a tight, polarized Caco2/TC7 monolayer, cells transfected with either CT or drebrin siRNA were grown on permeable supports for 5 days, after which epithelial cell polarity and TJ formation and function were assessed (see Materials and Methods). Despite the substantial decrease observed in the drebrin E levels, no epithelial cell polarity defects were detected in Caco2/TC7 cells. Both villin, a marker of apical microvilli, and the dipeptidyl peptidase DPPIV, an apical hydrolase, were still present at the apical pole of the cells, whereas scribble (Scrib) and E cadherin were both found to be present in the lateral membrane, as in the CT cells (Fig. 1B). Occludin (Occ), a marker of TJs (Fig. 1B, arrowheads), was observed forming a complete belt in both CT and drebrin E KD cells (supplementary material Fig. S4A), whereas no significant functional changes in the junctions were detected upon measuring the trans-epithelial resistance (TER) of CT and drebrin E KD monolayers (supplementary material Fig. S2B). All these data show that neither epithelial cell polarity nor TJ function was affected by drebrin E depletion. TJ formation might have been triggered and completed before day 3, however, when the process of drebrin E depletion was less advanced (supplementary material Fig. S2A). To overcome this problem, a calcium switch experiment adapted for use with Caco2 cells was performed (see Materials and methods). Four hours after Ca^{2+} was added (Fig. 1C), ZO1, a marker of TJs, formed belt-like structures in both control and drebrin E KD cells, which indicates that normal TJ assembly occurs even after drebrin E depletion.

Interestingly, *X–Z* confocal sections showed that the elongation of the control cells had already started to occur on the apical-to-basal axis within 4 hours, as shown by the fact that ZO1 was localized in the apical region, whereas this was not observed in drebrin E KD cells, which remained flattened (Fig. 1C). Upon measuring the height of the monolayer in cells treated with drebrin E siRNA for 5 days (Fig. 1B,D), it was observed that these cells were ~50% shorter than the CT cells, whereas their overall cross-sectional area had increased nearly fourfold in comparison with that of the control cells (Fig. 1D). The average volume of the drebrin E KD Caco2/TC7 cells was calculated (see Materials and methods) and found to be 1.8 times greater than that of the CT cells. This change in morphology is not due to a difference in cell density that can be observed between CT and drebrin E KD cells as drebrin-E-positive and -negative cells still have different heights when contacting each other (supplementary material Fig. S3). Therefore, although the loss of drebrin E does not seem to affect several visible aspects of apico-basal polarity in Caco2/TC7 cells, its elimination nonetheless impairs the ability of the cells to lengthen appropriately when the cells start to be compacted during the differentiation process.

The apical F-actin network is disrupted in Drebrin E KD cells

As drebrin expression in the developing brain has been described as a dynamic process (reviewed by Dun and Chilton, 2010), drebrin E localization was monitored in Caco2/TC7 cells from days 2 to 7. Between days 3 and 5, Caco2/TC7 cells begin to undergo the final differentiation processes, resulting in the specialization of the apical membrane and the formation of a terminal web and a dense brush border (Peterson and Mooseker, 1992). During this period, we noted that the intracellular localization of drebrin E changed from being mostly cortical in the lateral membrane to strongly subapical in the TJ or apical region of the cells while keeping a lateral contribution, in a similar way to F-actin (Fig. 2A,B, CT panels). This subapical accumulation varied from cell to cell, probably depending on the state of differentiation reached by each individual cell at day 5.

Drebrin is an F-actin-binding protein (Asada et al., 1994), and the drebrin E KD cell-elongation defects observed here are consistent with the notion that this protein affects the pattern of F-actin distribution in the apical region of Caco2/TC7 cells. The F-actin networks were therefore monitored in CT and KD Caco2/TC7 cells on day 3, just before the occurrence of the compaction

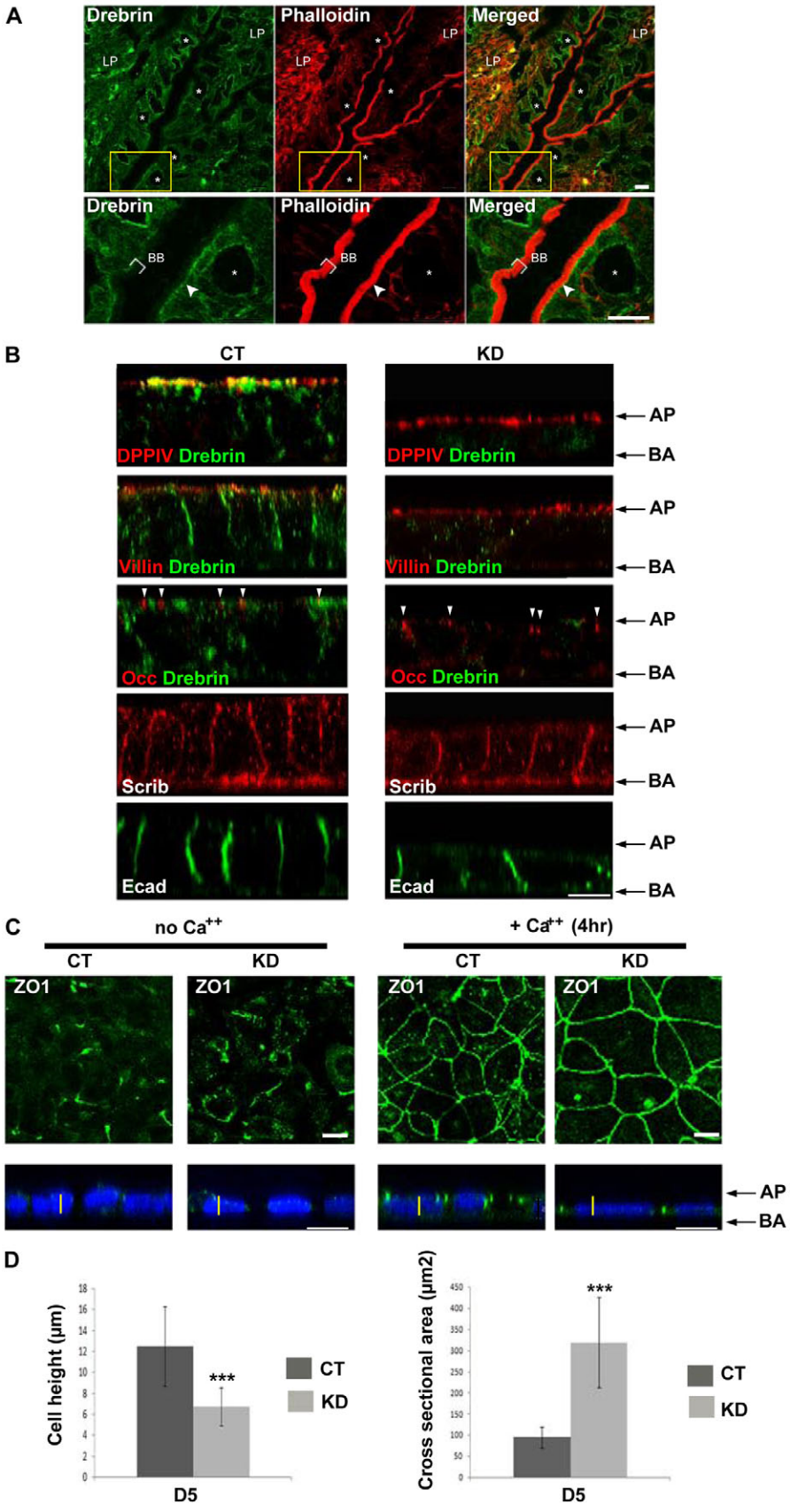

Fig. 1. Drebrin E is necessary for a columnar epithelial cell shape to develop. (**A**) Localization of drebrin E in human intestinal tissue. The top row shows semi-thin sections of human duodenum labeled with guinea pig antibodies against drebrin (in green) and with Texas-Red–phalloidin for F-actin (in red). The bottom row is a higher-magnification of the apical region of two villi (as delineated by the yellow rectangle in the top row). The arrowhead indicates the position of the terminal web, goblet cells are indicated by asterisks, and the brush border (BB) thickness is indicated by brackets. LP, lamina propia; scale bar: 10 µm. (**B**) Depletion of drebrin E prevents apico-basal elongation without affecting cell polarity. Localization of apical and basal markers on *X–Z* section images of control (CT, left panels) and drebrin knockdown (KD, right panels) cells. Shown are the localizations of DPPIV (apical marker), villin (marker of microvillar actin), occludin (Occ; a marker of tight junctions), drebrin E, scribble (Scrib) and E-cadherin (Ecad) (markers of the basolateral membrane). Black arrows indicate the top (AP, apical) and bottom (BA, basal) of the cell monolayer, and white arrowheads point to tight junctions. Scale bar: 10 µm. (**C**) Depletion of drebrin E does not affect the formation of tight junctions. Control (CT) or Caco2 cells depleted of drebrin E (KD) were grown in low-Ca^{2+} medium overnight ('no Ca^{2+}'), and reassembly of junctions (followed by ZO-1 staining) was triggered by adding Ca^{2+} for 4 hours ['+Ca^{++} (4hr)']. Arrows indicate the top (AP, apical) and the bottom (BA, basal) of the cell monolayer. Yellow vertical lines correspond to a length of 5 µm; white scale bar: 10 µm. (**D**) Histograms give the cell height (left) and the cross-sectional area (right) of CT and drebrin E KD cells. Cell height (n=92 cells) and cross-sectional area (n=160 cells) are presented together with the means ± s.d. Asterisks signify significant differences between CT and drebrin E KD cells (P≤0.001).

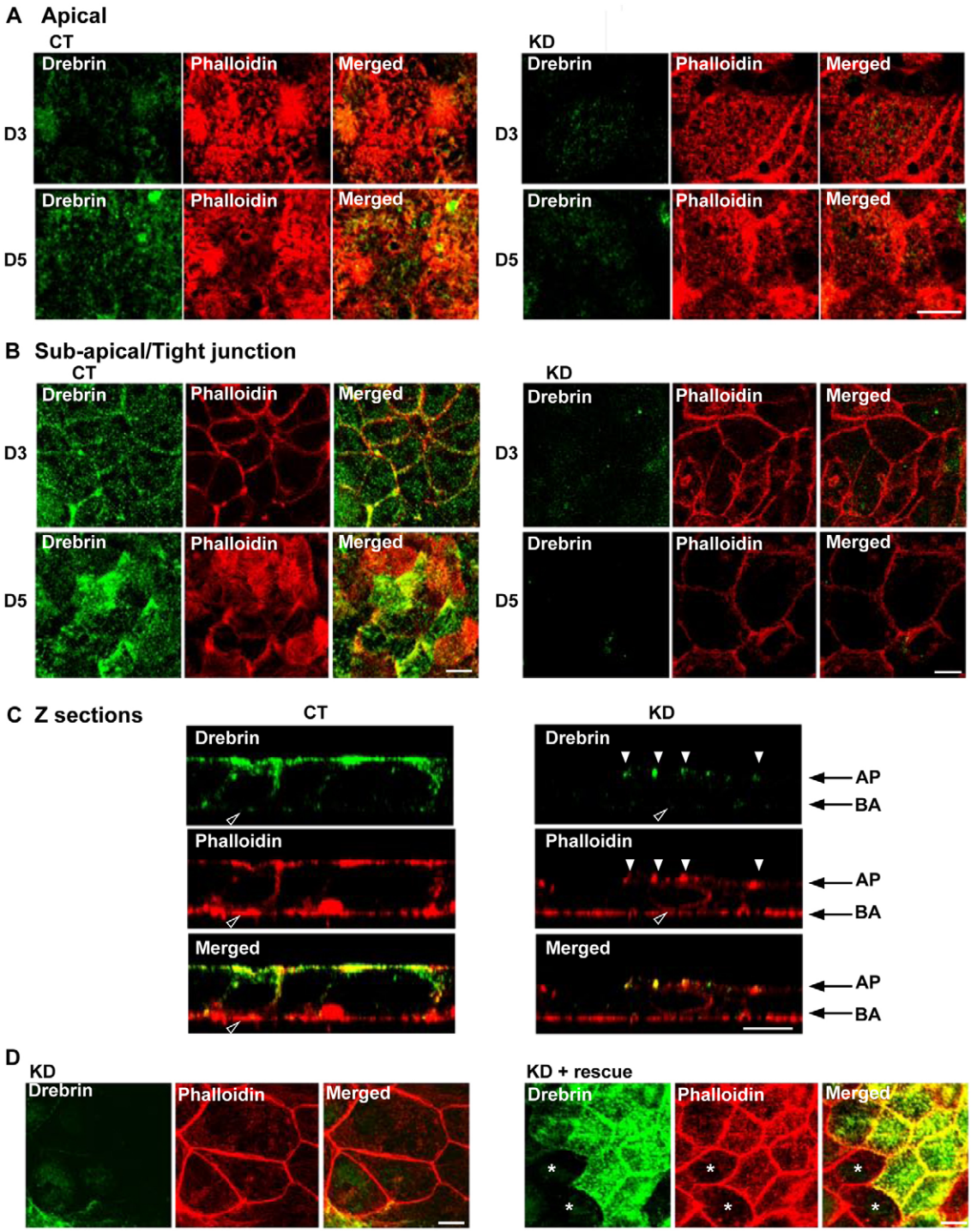

Fig. 2. The actin network is disrupted by drebrin E depletion and rescued by heterologous drebrin E expression. Drebrin E (in green) and F-actin (Texas-Red–phalloidin, in red) labeling in control (CT) and Caco2 cells depleted of drebrin E (KD) after 3 (D3) and 5 (D5) days of growth on filters. *X–Y* confocal sections were acquired at the apical pole (**A**) or at the level of the terminal web (subapical) of the cells (**B**). Scale bar: 10 μm. (**C**) Localization of drebrin E (in green) and F-actin (Texas-Red–phalloidin, in red) on *X–Z* confocal sections of control (CT) or Caco2 cells depleted of drebrin E (KD) after 5 days of growth on filters. Black arrows indicate the top (AP, apical) and the bottom (BA, basal) of the cell monolayers. Scale bar: 10 μm. Filled arrowheads indicate apical F-actin, and empty arrowheads point to basal F-actin. (**D**) Mouse drebrin E rescues apical F-actin accumulation**.** *X–Y* confocal sections performed at the level of the terminal web of cells transfected with human drebrin E siRNA (KD) or human drebrin E siRNA plus mouse drebrin cDNA ('KD + rescue'). Asterisks indicate drebrin E KD cells. Scale bar: 10 μm.

and elongation processes, and subsequently on day 5, after the brush border started to be formed by the cells. *X–Y* confocal sections were performed at the most apical level, where microvilli occur (Fig. 2A), and at the subapical level, where the terminal web and TJs are formed (Fig. 2B; supplementary material Fig. S4).

At the subapical level (which was labeled by occludin accumulating in the TJs) (Fig. 2B; supplementary material Fig. S4), a dramatic change in the patterns of distribution of both drebrin E and F-actin occurred in CT cells between days 3 and 5. Both proteins showed a strong lateral cortical labeling on day 3, with little accumulation at the apical pole of the cells. At this stage, the pattern of expression of these two proteins overlapped, although, unlike F-actin, drebrin E did not form a complete belt around the cells. By day 5, in CT cells, drebrin E and F-actin had accumulated densely in the terminal web network in the subapical cytoplasm in addition to their lateral localization (Fig. 2B; supplementary material Fig. S4). This strong subapical accumulation of F-actin was not observed in drebrin E KD cells, and the fluorescence intensity of phalloidin–Texas-Red at the subapical level was found to be only 7.6% of that of CT cells (see Materials and Methods). The fact that the increase in the F-actin levels in the terminal web was blocked in drebrin E KD cells (Fig. 2B) indicates that drebrin E is a prerequisite for the formation or stabilization of the subapical F-actin network involved in the formation of the terminal web.

X–Z sections were also analyzed on day 5, and an apical pattern of accumulation of drebrin E was observed in many CT cells, along with a strong colocalization with F-actin, which suggests the occurrence of interactions between apical F-actin and drebrin E (Fig. 2C). In KD cells, this F-actin signal present at

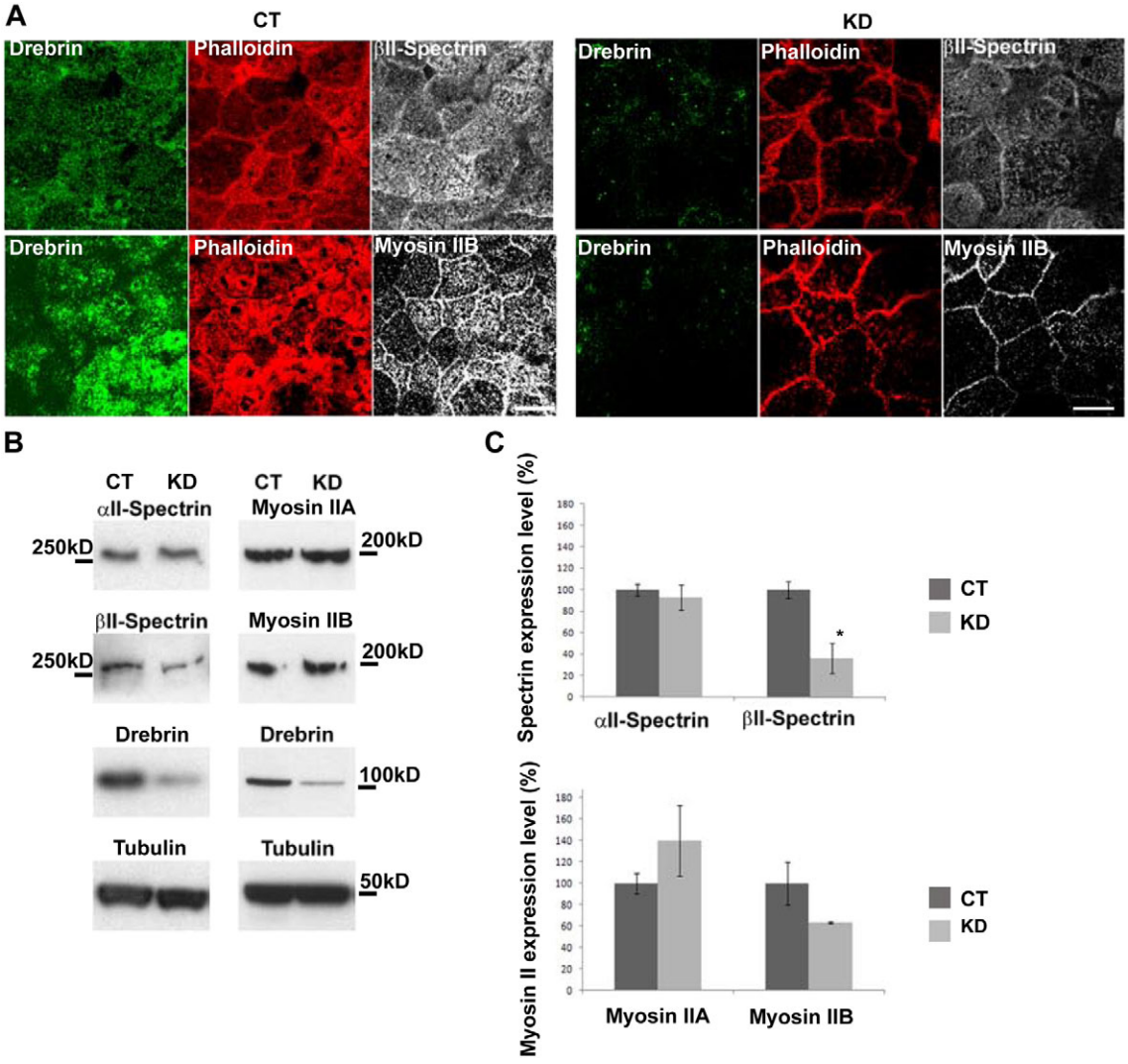

Fig. 3. The proper apical localization of proteins in the terminal web depends on the presence of drebrin E. (**A**) *X–Y* confocal sections of the subapical region (corresponding to the terminal web) of control (CT) and Caco2 cells depleted of drebrin E (KD) immunostained to detect drebrin E (in green), F-actin (Texas-Red–phalloidin, in red) and βII-spectrin (in white), or drebrin E (in green), F-actin (Texas-Red–phalloidin, in red) and myosin IIB (in white). Scale bar: 10 μm. (**B**) Immunoblot analysis showing the levels of expression of αII-spectrin, βII-spectrin (left panels), and myosin IIA, IIB (right panels) in drebrin E knockdown (KD) and control Caco2 cells (CT) of two different experiments. α-Tubulin was used to standardize the loading conditions in both cases. Histograms show the levels of expression of αII-spectrin, βII-spectrin (top panel) and myosin IIA and myosin IIB (bottom panel) on CT or drebrin E KD cell lysates. Data are mean values obtained in three experiments ± s.d. The asterisk signifies a significant difference between CT and drebrin E KD cells ($P \leq 0.05$).

the apical side of the cells was lost, except in a few areas, where some remaining drebrin E was also observed (Fig. 2C, solid arrowheads), which further supports the finding that subapical drebrin E contributes crucially to F-actin accumulation. It is worth noting that, although most of the apical F-actin was lost in drebrin E KD cells, the basal F-actin was still present in the stress fibers formed in KD cells (Fig. 2C, empty arrowheads) (supplementary material Fig. S4C).

To confirm whether the effects observed on the pattern of apical actin expression were specifically due to drebrin E KD, transient rescue experiments were performed using mouse drebrin E cDNA in human drebrin E KD cells. Expression of mouse drebrin E was allowed to occur for 2 days after a 3-day treatment with siRNA against human drebrin E (see Materials and Methods), and cells with and without mouse drebrin E were analyzed by performing confocal microscopy. In cells expressing high levels of mouse drebrin E, the F-actin network was restored in the subapical region of the cell [as determined by occludin labeling (data not shown)], which shows that drebrin E was indeed directly responsible for the loss of subapically accumulating actin filaments (Fig. 2D). The recovery of cell elongation processes could not be observed, however, probably because of the time-frame used in the experiment (2-day mouse drebrin E expression) as overexpression of mouse drebrin E for more than 2 days is deleterious to Caco2 cells (data not shown).

Drebrin E regulates spectrin and myosin IIB accumulation in the terminal web

To investigate more closely how drebrin E affects the formation and the structure of the terminal web, the levels of spectrin, a key protein complex expressed in the terminal web, were monitored. The spectrin complex comprises two subunits, αII spectrin and βII spectrin, both of which bind to actin (Glenney et al., 1982; Mooseker and Tilney, 1975; Peterson and Mooseker, 1992). Using antibodies against βII spectrin on day 5 in CT and KD cells, drebrin E and βII spectrin were found to be concentrated with F-actin located in the terminal web of CT cells (Fig. 3A), whereas the βII spectrin staining intensity was much lower (39.6% when compared with that of CT cells) in drebrin E KD cells (Fig. 3A). The results of western blot analysis showed that the level of βII spectrin expression in drebrin E KD cells was only 34% ±5.5 (s.d.) in comparison with that of CT cells (Fig. 3B), in line with the immunofluorescence data, which suggests that drebrin E specifically affects the expression and/or the stability of βII spectrin, in addition to its effects on the accumulation of F-actin in the subapical domain. To distinguish between a decrease in biosynthesis or an increase in degradation (or both), we measured the levels of newly synthesized βII spectrin after a metabolic pulse and a chase of either 0 or 16 hours (see Materials and Methods). We indeed found a clear decrease (~50%) in the biosynthesis of βII spectrin but no obvious increase in degradation in drebrin-E-depleted cells when compared with CT cells (data not shown). Surprisingly, neither the levels of expression of αII spectrin nor its pattern of distribution were affected by drebrin E depletion, indicating that different mechanisms control the levels of these two proteins (Fig. 3B; supplementary material Fig. S6C).

Myosin II has been reported to play a major role in apical constriction and the occurrence of epithelial cell rearrangements (Bertet et al., 2004). Two different isoforms of myosin II (myosin IIA and myosin IIB) are expressed in the terminal web (Heintzelman et al., 1994; Peterson and Mooseker, 1992). In our hands, only antibodies directed against myosin IIB produced a specific signal in Caco2/TC7 cells (data not shown). In polarized CT cells grown for 5 days on filters, the myosin IIB staining formed a complete belt around the cell cortex, as well as a dense pattern of cytoplasmic dots in the subapical region of the cells (Fig. 3A). Drebrin E depletion affected myosin IIB distribution as a loss of subapical accumulation was observed (27.9% when compared with the fluorescence intensity of CT cells), whereas the lateral cortical region of staining persisted, where myosin IIB was colocalized with F-actin (Fig. 3A).

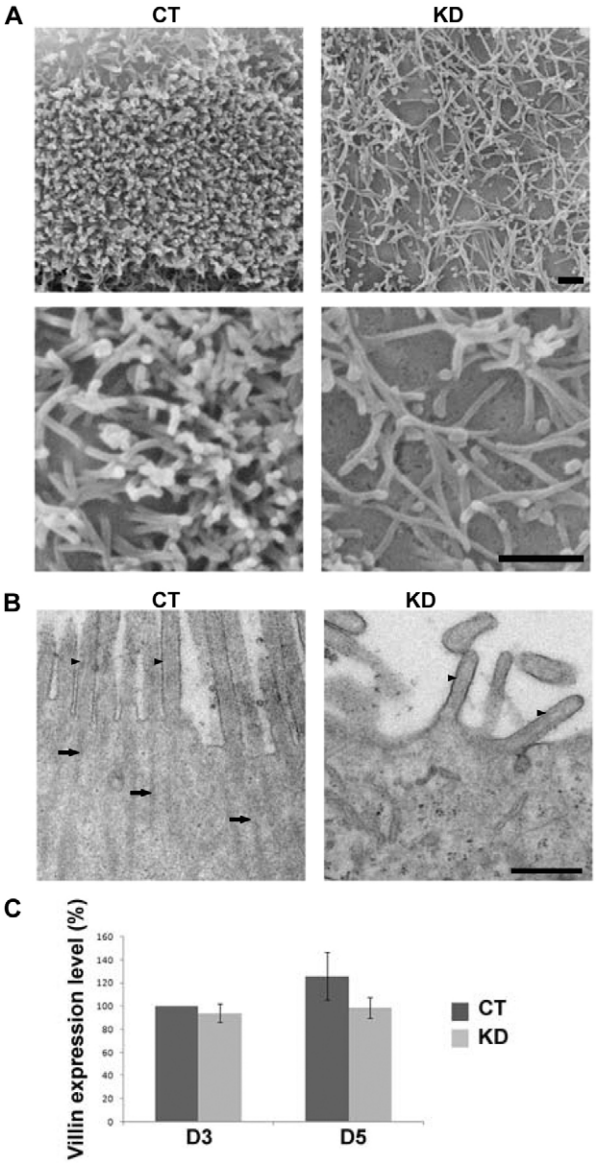

Fig. 4. The proper apical organization of intestinal cells requires drebrin E. (**A**) Scanning electron microscopy images of the apical surface of control (CT) and Caco2 cells depleted of drebrin E (KD) at 5 days after transfection. Scale bars: 1 μm. (**B**) Transmission electron microscopy images of the apical region of control (CT) and Caco2 cells depleted of drebrin E (KD) at 5 days after transfection. Arrows indicate microvillar actin rootlets in the subapical region of the cell. Arrowheads indicate apical microvilli. Scale bar: 0.5 μm. (**C**) Levels of villin expression on CT or KD cell lysates. Data are mean values obtained in three experiments ± s.d.

Quantitative analysis of myosin IIA and IIB showed that, in drebrin E KD cells, the expression levels of myosin IIB decreased significantly (63±15% in comparison with those of CT cells), whereas the levels of myosin IIA increased under the same conditions (143±33% in comparison with those of CT cells) (Fig. 3B). This decrease in the myosin IIB levels was correlated with the strong disappearance of this protein from the subapical region, where the terminal web structure would normally be established. Drebrin E expression is therefore necessary for the appropriate process of accumulation of both βII spectrin and myosin IIB to occur in the terminal web. By contrast, βII spectrin depletion did not affect the subapical accumulation of drebrin E,

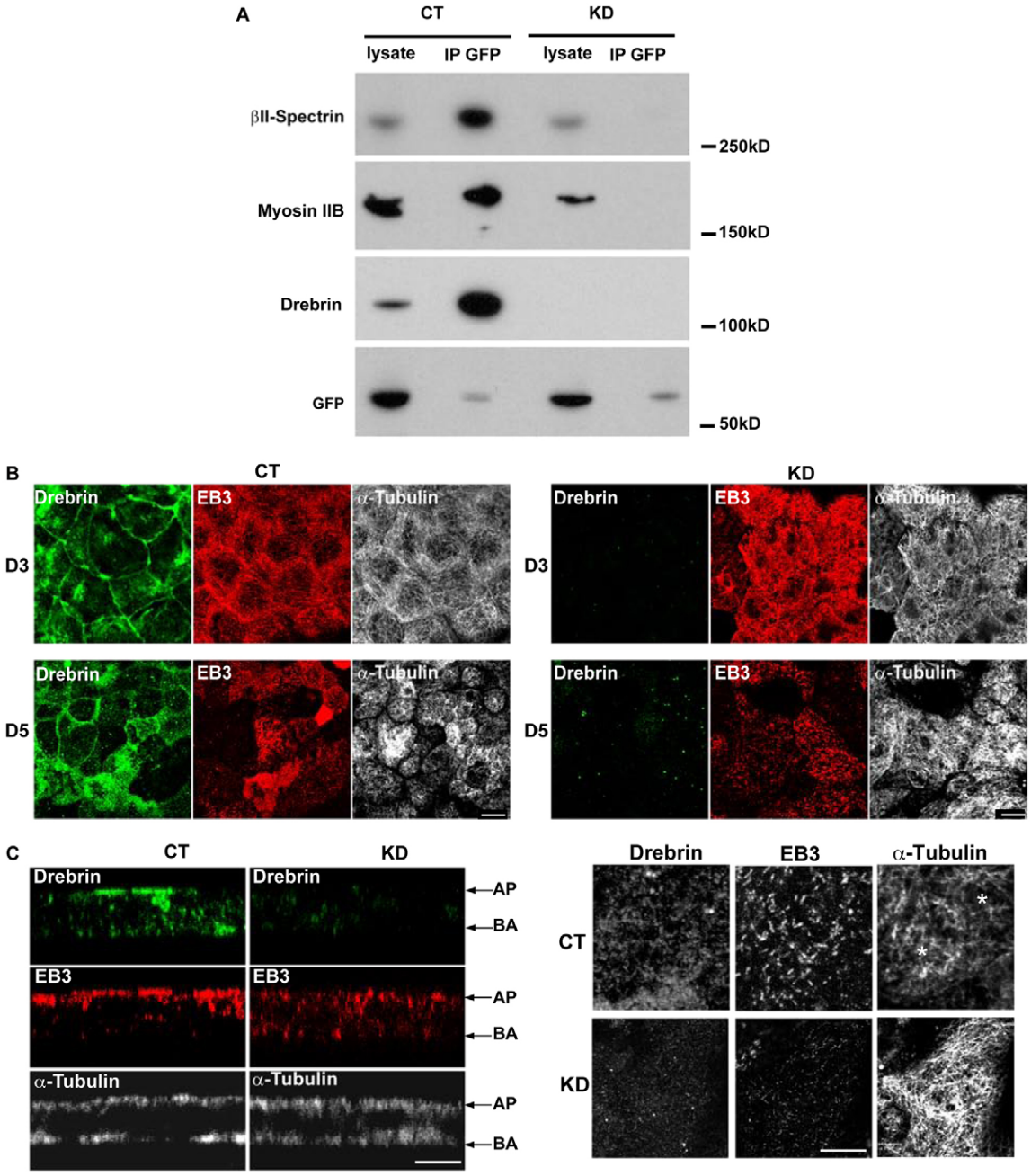

Fig. 5. Drebrin E interacts with EB3 and is necessary for the apical accumulation of EB3 to occur in Caco2 cells. (**A**) Caco2 cells stably expressing EB3–GFP were transfected with control siRNA (CT) or drebrin E siRNA (KD). Cell lysates were immunoprecipitated with antibodies against GFP ('IP GFP') and probed to detect the presence of βII-spectrin, myosin IIB or drebrin E. Molecular mass is indicated in kilodaltons. (**B**) Immunolabeling for drebrin E (in green), EB3 (in red) and α-tubulin (in white) in control (CT) and Caco2 cells depleted of drebrin E (KD) after 3 (D3) and 5 (D5) days of growth on filters. *X*–*Y* confocal sections were acquired at the apical pole of the cells. Scale bar: 10 μm. (**C**) Localization of drebrin E (in green), EB3 (in red) and α-tubulin (in white) on *X*–*Z* (left panels) or *X*–*Y* (right panels) confocal sections of control (CT) and Caco2 cells depleted of drebrin E (KD) after 5 days of growth on filters. Arrows indicate the top (AP, apical) and the bottom (BA, basal) of the cell monolayers. Scale bar: 10 μm. Cells were fixed with methanol, which flattens both CT and drebrin E KD cells. Asterisks indicate two individual cells.

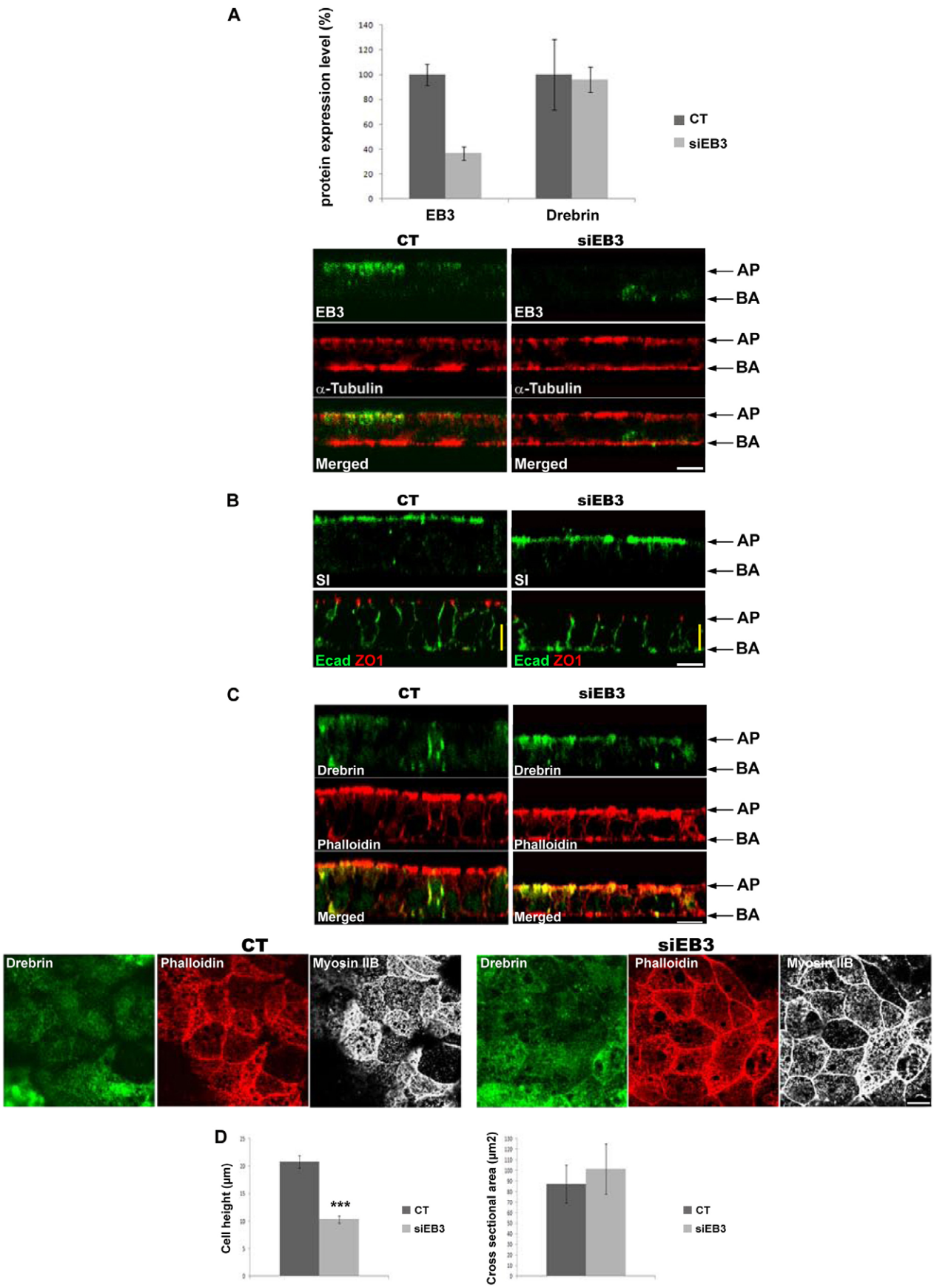

Fig. 6. See next page for legend.

F-actin or myosin IIB (supplementary material Fig. S5B). These data indicate that drebrin E acts along with F-actin upstream of βII spectrin, localizing βII spectrin and myosin IIB at the subapical level and thus promoting the formation and the function of the terminal web in the intestinal columnar epithelia.

Brush border formation requires drebrin E

The formation of the intestinal brush border depends on the correct assembly of an apical F-actin cytoskeleton. The expression of the key proteins required for brush border formation was therefore investigated, in addition to the morphological appearance of the developing brush border after its differentiation. Villin was used as a marker of microvillar actin as it has been established that villin contributes to forming the cytoskeleton of microvilli by crosslinking actin bundles (Bretscher and Weber, 1979). Despite the conspicuous disruption of the apical actin network, the typical apical villin staining levels increased in drebrin E KD cells between days 3 and 5 (supplementary material Fig. S6) and the overall level of villin expression was not significantly affected (Fig. 4C), which indicates that at least some microvilli did in fact form.

Scanning electron microscopy (SEM) findings obtained on polarized control and KD cells grown for 5 days after siRNA transfection indicated that, in comparison with the microvilli present in the dense brush border of CT cells, which were found to be erect and packed together in bundles (Fig. 4A), the microvilli of drebrin E KD cells were much less dense and did not form a well-organized brush border: they were lying flat on the apical surface of the cells and showed variable degrees of branching (Fig. 4A). Morphological studies using transmission electron microscopy (TEM) showed that the rootlets anchoring microvilli to the terminal web, as well as the terminal web itself, were almost undetectable in drebrin E KD cells (Fig. 4B). In addition, the fact that the subapical region was invaded by rough-endoplasmic-like structures further supported the idea that the terminal web was greatly disorganized. Brush border development parallels the expression of typical transmembrane enzymes from the intestine such as DPPIV and sucrase-isomaltase (SI) (Rousset, 1986). We thus quantified the expression of DPPIV and SI in CT and drebrin E KD Caco2/TC7 cells 5 days after siRNA transfections. We noted a significant decrease in the expression levels of both DPPIV [69% ±16 (s.d.) of CT] and SI [44% ±20 (s.d.) of CT] in drebrin E KD cells compared with those of CT cells, whereas E-cadherin, a basolateral adhesion protein, was unaffected (data not shown). The differences observed for the total amount of protein expression could be explained by a decrease in protein synthesis and/or an increase in protein degradation caused by the loss of drebrin E. To address this question, we used a pulse–chase assay combined with immunoprecipitations (Rodriguez-Boulan et al., 1989) performed with DPPIV and SI. Quantitative analyses of the different immunoprecipitates indicated that the synthesis of both proteins was reduced in drebrin KD cells compared with that of the CT cells (65 and 75% of reduction, respectively), whereas protein degradation remained unchanged (data not shown). These data show that the integrity of the subapical actin cytoskeleton involved in the formation and terminal differentiation of the brush border depends on the presence of drebrin E.

Drebrin and EB3, a plus-end microtubule-binding protein, form a complex and are both required for apico–basal elongation

It has been observed that, in fully polarized Caco2 cells, a dense microtubular network runs parallel to the apical, and down the lateral, membranes (Gilbert et al., 1991), providing a potential scaffold for cell elongation processes. Interestingly, it was recently reported that drebrin E binds to EB3 and tethers F-actin and microtubules in the growth cone (Geraldo et al., 2008). In order to confirm the occurrence of this interaction, Caco2/TC7 cells were stably transfected with an EB3–GFP construct (Stepanova et al., 2003). This construct mimics the endogenous distribution of EB3 (Fig. 5B,C; and data not shown), and the GFP-tag was used to immunoprecipitate EB3–GFP and its potential partners. Drebrin E was greatly enriched in the immunoprecipitate, and myosin IIB and βII spectrin were also co-immunoprecipitated, which showed the existence of a complex containing at least these four proteins. When the same immunoprecipitation procedure was performed using EB3–GFP, in Caco2 cells depleted of drebrin E, neither myosin IIB nor βII spectrin was precipitated by EB3–GFP, which provides evidence that drebrin E is essential to the formation of this complex (Fig. 5A). To determine the effects of this EB3–drebrin-E interaction, the localizations of microtubules, drebrin E and EB3 were investigated in CT and drebrin E KD cells on day 5 during the cell elongation process. The microtubules, drebrin E and EB3 all accumulated in the subapical region of the CT cells (Fig 5B, left). The subapical accumulation of EB3 and microtubules can be clearly observed in the *X–Z* confocal sections (Fig. 5C). In drebrin KD cells, however, EB3 was more randomly distributed along the apico-basal axis, whereas a microtubule network was still present on the apical side using both *X–Y* and *X–Z* confocal sections (Fig. 5B,C), whereas quantitative analyses on western blots showed that total EB3 protein levels were not affected by drebrin E depletion (data not shown). These data suggest that drebrin E is involved in the apical accumulation of EB3 during the basal to apical cellular elongation phase. By contrast, downregulation of EB3 affected neither the steady-state levels of drebrin E nor its localization (Fig. 6A), and it

Fig. 6. EB3 depletion affects cell elongation without perturbing cell polarity, cell compaction or terminal web formation. (**A**) Levels of EB3 and drebrin E expression in CT- and EB3- depleted (siEB3) cells expressed as percentages of the values obtained in control (CT) cells. Data are means of values obtained in three experiments ± s.d. *X–Z* confocal sections of CT and EB3-depleted (siEB3) Caco2 cells grown on filters for 5 days, methanol fixed and immunostained against EB3 (in green) and α-tubulin (in red). Arrows indicate the apical (AP) and basal (BA) poles of the cell monolayers. Scale bar: 10 μm. (**B**) Pattern of SI (in green, top row), ZO1 (in red, bottom row) and anti-E-cadherin (in green, bottom row) distribution in control (CT) and EB3-depleted cells (siEB3) grown for 5 days and fixed in paraformaldehyde. Arrows indicate the apical (AP) and basal (BA) poles of the cell monolayers. Scale bar: 10 μm. Note that siEB3 cells are not as high as CT cells (yellow vertical scale bar: 10 μm). (**C**) *X–Z* confocal section of control (CT) and EB3-depleted (siEB3) cells labelled to detect drebrin E (in green) and F-actin (Texas-Red–phalloidin, in red) (top row). Arrows indicate the apical (AP) and basal (BA) poles of the cell monolayers. Scale bar: 10 μm. The bottom row shows *X–Y* confocal sections at the level of the terminal web, labeled to detect drebrin E (in green), F-actin (Texas-Red–phalloidin, in red) and myosin IIB (in white) in Caco2 cells transfected with CT siRNA and EB3 siRNA (siEB3). Scale bar: 10 μm. (**D**) Cell height (left) and cross-sectional area (right) measured in CT and EB3-depleted cells (siEB3). Cell height (n=65 cells) and cross-sectional area (n=160 cells) are expressed as means ± s.d., and asterisks mark the existence of significant differences between CT and drebrin E KD cells ($P \leq 0.001$).

did not affect the distribution of an apical protein (SI), a TJ protein (ZO1) or basolateral E-cadherin (Fig. 6B).

The fact that actin filaments and drebrin E accumulation were still observed in the subapical region of the EB3-depleted cells (Fig. 6C) suggests that EB3 is not required for the formation of the terminal web. To confirm this point, the distribution of myosin IIB and drebrin E was studied in *X–Y* confocal sections after EB3 depletion. No significant differences were observed between CT- and EB3-depleted cells, and drebrin E, F-actin and myosin IIB still formed a subapical network (Fig. 6C). Although the polarity and the terminal web were not perturbed, it is worth noting that the overall morphology of the EB3-depleted cells was abnormal. EB3-depleted cells were 10 µm ± 1.8 (s.d., $n=92$) in height, as opposed to 21 µm ± 3.8 (s.d., $n=92$) in the case of CT cells. By contrast, the cross-sectional areas did not differ significantly between EB3-depleted and CT cells (Fig. 6D). EB3 is therefore required for cell elongation but not for cell compaction, whereas drebrin E is required for both.

All these data strongly suggest that drebrin E is needed for the accumulation of EB3 in the subapical region of Caco2/TC7 cells prior to the process of apico-basal elongation. In addition, drebrin E is required for the formation of the F-actin-based terminal web, where it is necessary for myosin IIB and βII spectrin accumulation, thus promoting the EB3-independent process of cell compaction. Importantly, the presence of an intact terminal web does not suffice to promote cell elongation, which requires the apical microtubule network to be connected to the terminal web by EB3 (see model in Fig. 7).

Discussion

Although the expression of drebrin has been studied previously in neurons and its possible functions have been discussed, the present findings unexpectedly suggest that drebrin E might be an actin-binding protein that makes a crucial contribution to the typical changes in cell shape that occur during the process of epithelial morphogenesis. The presence of drebrin E is essential for cells to be able to lengthen along the apico-basal axis and for the terminal-web-promoting apical contraction and differentiation to be executed. Drebrin E interacts with EB3, as well as determining the pattern of distribution of the latter protein. In addition, the contribution of drebrin E to the apico-basal cell elongation process depends on the presence of EB3, which suggests that, as in the growing axon, these two proteins form connections between the F-actin and microtubule networks in the subapical region of columnar epithelial cells.

Drebrin E contributes to regulating the subapical F-actin network

The accumulation of drebrin E at the subapical level was found to be concomitant with the redistribution of F-actin, based on the strong cortical staining observed at the level of the tight junctions, with a dense network underlying the apical membrane known as the terminal web (Mooseker and Tilney, 1975). Drebrin E depletion prevented this re-distribution of F-actin from occurring, and the disruption of the terminal web probably accounts for the defects in the brush border observed as microvilli were still formed, but they were unable to project their

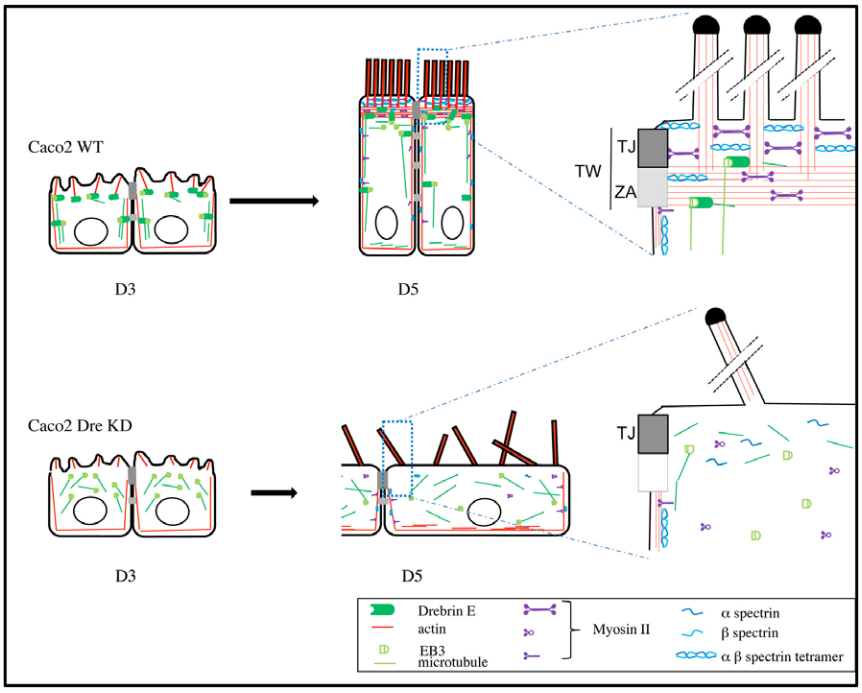

Fig. 7. A model for the potential role of drebrin E in the organization of the subapical F-actin network and during cell elongation. Cartoon of control (WT) and Caco2 cells depleted of drebrin E (Dre KD) after 3 (D3) and 5 (D5) days of growth on filters at confluence. At day 3, no obvious morphogenetic defect can be detected, whereas, at day 5, the subapical F-actomyosin network associated with the zonula adherens (ZA) is not present owing to the lack of subapical drebrin accumulation. This lack of terminal web (TW) in Dre KD cells prevents the anchoring of microvilli roots as opposed to WT cells. This absence of a subapical actomyosin network is probably responsible for the compaction defect. In addition, apico-basal elongation in Dre or EB3 KD cells is impaired, and this could be the consequence of the lack of connection and/or cooperation between the F-actomyosin apical network and the apico-lateral microtubule network through the interaction between drebrin E and EB3. TJ, tight junction. Illustration based on the structure of the TW as described by Mooseker (Mooseker, 1985).

rootlets into the missing dense F-actin network. Drebrin E directly promotes the subapical accumulation of F-actin as F-actin still accumulated in regions where drebrin E was still present (Fig. 5C). When no subapical F-actin was present, proteins such as myosin IIB or β-spectrin, which crosslink and connect F-actin bundles, were strongly diminished subapically too. The exact effects of drebrin E on the F-actin network have not yet been elucidated, and drebrin shows no actin-severing, -nucleating or -bundling activity in vitro (Ishikawa et al., 1994). It has been established, however, that drebrin A attenuates the interactions between F-actin and myosin V in vitro (Ishikawa et al., 2007), and drebrin E might therefore antagonize the interactions between F-actin and myosin IIB in a similar way. Depletion of drebrin E disrupted the F-actin and myosin IIB networks subapically, but not cortically, at the level of the tight junctions, which shows that the interactions between F-actin and myosin IIB were not generally disrupted in drebrin E KD cells. The presence of drebrin E is necessary, however, for normal cellular levels of both βII spectrin and myosin IIB to occur. The fact that drebrin E, β-spectrin and myosin IIB were detected in the same immunoprecipitate is consistent with the possibility that these three proteins might form a macromolecular complex in the TW.

Contribution of drebrin E to apical morphology

Drebrin KD Caco2/TC7 cells were larger and flatter than CT cells, possibly because no apico-basal elongation and apical constriction occurred in these cells at a time when the cell-compaction process normally occurs. In CT cells, both drebrin E and F-actin, which are mainly present cortically around the lateral membrane, are redistributed to the subapical part of Caco2/TC7 cells during this compaction process. When this redistribution of F-actin was prevented by depletion of drebrin E, the myosin IIB no longer accumulated in the subapical region of the cells. myosin IIB has been found to be essential for apical actin accumulation and cell compaction to occur during neural tube closure (Rolo et al., 2009). In drebrin E KD cells, myosin IIB was still associated with F-actin in the cortex of the lateral membrane, but, as there are no apical F-actin cables exerting tension forces, compaction cannot occur and the KD cells stay flat while remaining polarized. Here, it was established for the first time that drebrin E is essential for F-actin and myosin IIB to be properly distributed in the apical pole of polarized epithelial cells and that the presence of this drebrin-E–F-actin apical network is crucial for mammalian epithelial cells to be compacted into a columnar epithelium. Further studies should help to determine how drebrin E stabilizes both F-actin and myosin IIB in the terminal web and thus promotes the recruitment of proteins such as *βII* spectrin, which play a crucial role in the generation and/or maintenance of this structure. The presence of other actin-binding proteins, such as the shroom (Hildebrand, 2005) and lulu proteins (Nakajima and Tanoue, 2010), acting on the actomyosin network is also required for this columnar epithelial cell shape to develop, and it would be interesting to discover what the interplay between these proteins and the F-actin–drebrin-E–myosin-II complex involves.

The role of drebrin E in apico-basal elongation

In fully polarized Caco2 cells, a dense microtubular network runs parallel to the apical membrane and down to the lateral membrane (Gilbert et al., 1991), and it was established here that EB3, a microtubule-binding protein that interacts with drebrin E, is also enriched at the apical pole of differentiated Caco2 cells in a drebrin-E-dependent manner. The finding that there exists a drebrin-E-dependent complex consisting of EB3, drebrin E, myosin IIB and βII spectrin supports the idea that EB3–drebrin-E interactions link apical microtubules to the F-actin-based terminal web. Depletion of drebrin E might therefore disrupt both the subapical F-actin network, preventing both the formation of a terminal web and the EB3 link between F-actin and the apical microtubule network. This conclusion is further supported by the fact that EB3 depletion mimicked only part of the drebrin E KD phenotype in cells having an apical area similar to that of the control cells and showing no obvious lack of ability to express terminal web markers in the subapical area. A similar connection between microtubules and F-actin based on interactions between EB3 and drebrin E has also been described in growing axons (Geraldo et al., 2008), and decreasing the EB3 levels by applying RNAi treatment affected the spine-like shape by means of the actin cytoskeleton (Jaworski et al., 2009), which further supports the hypothesis that EB3 might determine cell shape and/or morphogenesis.

Two other proteins, shroom3 and DrhoGEF2, have been described as being possibly involved in the regulation of both the microtubules and the actomyosin network during the epithelial cell elongation processes. Shroom3 has been found to be involved in both apico-basal elongation and apical contraction in MDCK and neural epithelial cells, and this protein is necessary for γ-tubulin to be properly localized at the apical pole of epithelial cells in *Xenopus* embryos (Hildebrand, 2005; Lee et al., 2007). By contrast, DRhoGEF2 is involved in controlling not only the localization of apical myosin II but also the pattern of microtubule distribution through the apical accumulation of EB1 (an EB3-related protein) in *Drosophila* (Rogers et al., 2004), which suggests that DRhoGEF2 might act together or in parallel with the EB3–drebrin-E pathway. Future studies on the exact role of the connections formed between apical microtubules and the F-actin network during epithelial and apical morphogenesis and on how drebrin E controls the processes involved should shed light on how this protein affects the cytoskeletal network, resulting in changes in cell shape and eventually differentiation, which in turn reflect the activity of this protein during epithelial morphogenesis and development.

Materials and Methods

Cell culture

A Caco2 clone (TC7 cells) was grown as described previously (Chantret et al., 1994). Cells were transfected using the Amaxa device, T solution and the B-024 program (Amaxa Biosystems, Germany) by mixing 100 picomoles of siRNA with 100 µl buffer T and 1.5×10^6 freshly trypsinized cells in line with the manufacturer's instructions. Loss of drebrin expression was monitored using western blotting or immunofluorescence procedures. Caco2 cells were transfected with a plasmid encoding EB3–GFP (a gift from Anna Akhmanova) and selected with 2 mg ml^{-1} of G418 for two weeks. For TER measurements, cells (n=300,000) were seeded on Transwell filters (12 mm in diameter, Corning, NY), and TER was measured daily with a MilliCell apparatus (Millipore, Bedford, MA) in line with the manufacturer's instructions. Measurements obtained in the experiments shown in supplementary material Fig. S2 ranged from 167 Ωcm^2 ±25 (s.d.) to 203 Ωcm^2 ±23 (s.d.) with CT cells, from 152 Ωcm^2 ±13 (s.d.) to 199 Ωcm^2 ±11 (s.d.) with drebrin E KD cells.

Calcium switch experiments

For the Ca^{2+}-switch experiments, 1.5×10^6 TC7 cells cm^{-2} were grown overnight in Ca^{2+}-free D-MEM supplemented with 20% dialyzed FCS. Cell adhesion was then initiated by adding 1.8 mM $CaCl_2$ to the medium for 0 to 4 hours, and the cells were then fixed in 3% PFA and analyzed by immunofluorescence (Otani et al., 2006).

siRNA and cDNA

The following siRNA duplexes were used: human drebrin E siRNAs [D1: 5′-GCGGAUUAACCGAGAGCAGtt-3′ (sense) and 5′-CUGCUCUCGGUUAAUCCGCtt-3′ (antisense), D2: 5′-GCAGACUUUAGAAGCGGAAtt-3′ (sense) and 5′-UUCCGCUUCUAAAGUCUGCtg-3′ (antisense)], control siRNA [siluciferase 5′-CGUACGCGGAAUACUUCGAtt-3′ (sense), 5′-UCGAAGUAUUCCGCGUACGtt-3′ (antisense), human βII spectrin siRNAs (F29: 5′-GGCUUGACAAAAUCGAGAAtt-3′ (sense) and 5′-UUCUCGAUUUUGUCAAGCCat-3′ (antisense), F30: 5′-CGAUGUUACAAGAACGAUUtt-3′ (sense) and 5′-AAUCGUUCUUGUAACAUCGtg-3′ (antisense), F31: 5′-GCACAAGUUUUACCACGAUtt-3′ (sense) and 5′-AUCGUGGUAAAACUUGUGCag-3′ (antisense)], and human EB3 siRNAs [MAPRE3 1: 5′-GAGCAUGAAUACAUCCACAtt-3′ (sense) and 5′-UGUGGAUGUAUUCAUGCUCta-3′ (antisense), MAPRE3 2: 5′-GAACGUGACUUCUACUUAtt-3′ (sense) and 5′-UGAAGUAGAAGUCACGUUCct-3′ (antisense)]. The siRNAs were synthesized by Ambion Applied Biosystems. The mouse drebrin cDNA used in the rescue experiments was purchased from Origene.

Antibodies

The mouse mAb against βII spectrin was raised from a fusion of myeloma cells (X63-Ag 8.653), as described (Galfré and Milstein, 1981), with spleen cells from mice immunized with purified β-spectrin chains. Spectrin was purified from frozen rabbit lens membranes, as described previously (Aster et al., 1986). Hybridomas were screened by performing western and dot blotting with purified spectrin. The βII spectrin antibody is an immunoglobulin G1 that recognizes the βII spectrin chain in both the denatured and native conformations in western blotting and immunofluorescence procedures.

Spectrin purification

Rabbit lens membranes were prepared by disrupting decapsulated lenses in ten times their weight of buffer A containing 0.25 mM sucrose, 2 mM EGTA, pH 7.5, and 0.2 mM phenymethylsulfonylfluoride (PMSF) with ten strokes in a Dounce homogenizer at 4℃. Membranes were collected by centrifugation at 16,000 ***g*** for 10 minutes. The pellet was resuspended in buffer A, homogenized and centrifuged as above; this procedure was repeated twice. The pellet was resuspended with one volume of extraction buffer (buffer B: 0.2 mM EGTA, pH 8, 0.2 mM DTT, 0.2 mM PMSF) and stirred at room temperature for 1 hour. The suspension was then centrifuged at 15,000 ***g*** for 30 minutes at 4℃. Proteins in the supernatant were precipitated by adding CH_3COONa to a final concentration of 10 mM and the pH was adjusted to 5.5. After stirring the preparation at 4℃ for 30 minutes, the precipitated proteins collected by centrifugation were resuspended in a small volume of buffer C (10 mM Tris-HCl, pH 8, 1.5 M KI, 1 mM EDTA, 0.2 mM DTT and 10 mM sodium thiosulfate) and applied to a Sepharose 4BCL column (0.9 × 100 cm), equilibrated and eluted with buffer D (10 mM Tris-HCl, pH 8, 0.6 M NaCl, 1 mM EGTA, 1 mM EDTA, 0.2 mM DTT). Fractions beginning with the void volume were monitored to detect spectrin chains by performing SDS-PAGE and Coomassie staining. Peak fractions were dialysed overnight against the spectrin buffer (10 mM Tris-HCl, pH 8, 50 mM KCl, 10 mM $MgCl_2$, 1 mM EGTA, 0.2 mM DTT) and injected into Balb/c mice.

Antibody sources

The following primary antibodies were used: guinea pig polyclonal anti-drebrin was used for the immunofluorescence assays (Progen Biotechnik), mouse mAb anti-drebrin was used for western blotting (Medical and Biological Laboratories) and mouse mAb (7.1 and 13.1) anti-GFP (Roche) and chicken polyclonal anti-GFP (Aves Laboratories), rabbit polyclonal anti-ZO1 (Zymed Laboratories), mouse mAb anti-Occludin (Zymed Laboratories), mouse mAb anti-E-cadherin (BD Biosciences Transduction Laboratories), goat polyclonal anti-Scribble (Santa Cruz), rat mAb anti-DPPIV (for details, see Gorvel et al., 1991), mouse mAb D8B7 anti-αII-spectrin (AbCam), rabbit polyclonal anti-myosin IIA (Cell Signaling Technology), rabbit polyclonal anti-myosin IIB (Cell Signaling Technology), mouse mAb anti-alpha-tubulin (Sigma Aldrich), mouse mAb anti-villin (a gift from Daniel Louvard) and rat mAb anti-EB3 (KT36, Abcam) were used. F-actin was detected using a phalloidin-TRITC conjugate (Sigma Aldrich). 4,6-Diamidino-2-phenylindole dihydrochloride (DAPI, Sigma Aldrich) was used to label the nuclei.

Western blotting, pulse–chase and co-immunoprecipitation procedures

Caco2 cells were extracted using lysis buffer 1 (50 mM Tris, pH 8, 150 mM NaCl, 50 mM NaF, 2 mM EDTA, 0.5% NP40, 1 μg ml^{-1} antipain, 1 μg ml^{-1} pepstatin, 15 μg ml^{-1} benzamidine, 1 μg ml^{-1} leupeptin, 0.1 mM orthovanadate) or lysis buffer 2 (20 mM Tris, pH 7.5, 150mM NaCl, 1mM EDTA, 1mM EGTA, 25 mM sodium pyrophosphate, 1% Triton-X100, 1 μg ml^{-1} antipain, 1 μg ml^{-1} pepstatin, 15 μg ml^{-1} benzamidine, 1 μg ml^{-1} leupeptin, 0.1 mM sodium orthovanadate) and analyzed using western blotting procedures as described previously (Michel et al., 2005) with primary antibodies and the corresponding secondary antibodies coupled to peroxidase. To measure the levels of protein biosynthesis (βII spectrin, DPPIV, SI), Caco2 cells were grown on Transwell filters for 5 days after transfection and processed for metabolic labeling and immunoprecipitations as described previously (Rodriguez-Boulan et al. 1989). Immunoprecipitation steps were performed as described previously (Massey-Harroche et al., 2007), using GFP-coupled beads (Santa Cruz) or primary antibodies and protein-coupled beads (GE Healthcare). Bands were revealed using the LumiLight kit (Roche Diagnostics, Meylan, France) and quantified using the ImageQuant TL software program (Amersham Biosciences).

Cell immunofluorescence

Nearly confluent TC7 cells were seeded onto Transwell filters and maintained for 3–5 days in vitro. Cells were washed with PBS supplemented with 1 mM $MgCl_2$ and 10 μM $CaCl_2$, fixed with 3% paraformaldehyde for 10 minutes and permeabilized in 0.5% triton X-100 or 1% SDS or in 5 mM EGTA, 0.1% saponin for 20 minutes or not permeabilized (depending on the antibody used) for 10 minutes. For EB3 staining, the cells were fixed and permeabilized with cold methanol for 7 minutes at −20℃. Cells were blocked in 0.4% gelatine and 0.025% saponin for 1 hour before being incubated with primary antibodies overnight at 4℃. After being incubated with the appropriate fluorescence-conjugated secondary antibodies, they were washed and mounted in DABCO or Mowiol anti-fading reagent. Images were acquired with a Zeiss 510 Meta microscope using 63 × Plan-Apochromat 1.4 NA oil and 100 × Plan-Apochromat 1.4 NA oil objectives (Zeiss, Le Pecq, France). Images were analyzed using the ImageJ software program to measure the cell height and cross-sectional area and fluorescence intensity. Cell volume was calculated based on a cylinder shape according to the following formula: mean cell height × mean cell area = mean cell volume. Measurement of the height of the monolayer showed that KD cells were 6.8 μm ± 1.8 (s.d., n=92) tall, and 13 μm ± 3.8 (s.d., n=92) for CT cells. The cross-sectional area was 318 μm^2 ±106 (s.d., n=156) for KD cells in contrast to 94 μm^2 ±25 (s.d., n=156) for CT cells. Fluorescence intensity was measured at the subapical level on X–Y confocal sections using ImageJ and then expressed as mean fluorescence intensity per unit surface area. A minimum of 15 independent cells was recorded for each protein.

Human intestine immunofluorescence

Human intestinal samples were obtained from the extremities of surgically resected isolated cancerous tumors located in the caudal part of the ileum. These tissues were found to be normal upon histological examination. Small pieces of intestine were fixed for 4 hours in phosphate buffer containing 4% formaldehyde freshly prepared from paraformaldehyde. The fixed tissues were infused for 2 hours at room temperature in a 0.1 M phosphate buffer (pH 7.4) containing 2 M sucrose, and the fragments were then frozen in liquid nitrogen and sectioned in a Reichert Ultracut S/FCS device (Leica, Reichert Division, Wien, Austria). Sections of thickness 1 μm were picked up with a droplet of 2.2 M sucrose, as described previously (Tokuyasu, 1978) and deposited on a glass slide. After saturating nonspecific sites with 10% calf serum in PBS, immunofluorescence labeling was performed in the same way on both tissue sections and cells.

Statistical analysis

Data are expressed as means ± s.d. The Mann–Whitney U test was used for the statistical analyses.

Electron microscopy

SEM: TC7 cells grown on glass coverslips were fixed with 2.5% glutaraldehyde in 0.1 M cacodylate buffer (pH 7.4) for 1 hour, washed three times for 15 minutes in 0.1 M cacodylate buffer, post-fixed with 1% osmium tetroxide in cacodylate buffer for 1 hour at room temperature, washed for 15 minutes with the same buffer, dehydrated through a graded ethanol series: 25%, 50%, 70%, 85%, 90%, 100% for 15 minutes at room temperature, completed by hexamethyldisilizane (HMDS) steps (three sets of 1 hour each) and air-dried overnight under a fume hood. Finally, samples pasted on a specific SEM holder (Edwards sputter coater S150B apparatus) were coated with a thin layer of gold using ion sputtering methods. Samples were then examined under a Leica S440 scanning microscope (20 kV of accelerating voltage).

TEM: impregnated samples were embedded in Epon resin for 48 hours at 60℃. Ultrathin sections (80 nm) were obtained using a Leica Ultracut UCT microtome (Leica, Austria) equipped with a diamond knife (Drukker, The Netherlands). Sections were collected on a copper grid and stained with uranyl and lead citrate (Reynolds, 1963). Observations were performed on an EM 912 electron microscope (Zeiss, Germany) at a 100-kV accelerating voltage equipped with a BioScan model 792 camera (Gatan, USA).

Acknowledgements

We thank the Le Bivic laboratory members, Richard Roy (McGill University, Canada) for critical reading and discussions about this manuscript, the IBDML microscopy facility for live imaging

experiments and Jean-Paul Chauvin (IBDML) for the electron microscopy.

Funding

This research was supported by the CNRS (UMR 6216) and Université de la Méditerranée. The Le Bivic group is an 'Equipe labellisée 2008 de la Ligue Nationale contre le Cancer'. E.B. was the recipient of a fellowship from the French Ministry for Education and Research and Grant agreement [grant number HEALTH-F2-2008-200234]. This project was supported by Coordination Theme 1 (Health) of the European Community's FP7 Grant agreement [grant numbers HEALTH-F2-2008-200234, ANR Neuroscience DYOR and ANR n°BLAN07-2-186738 to A.L.B.].

Supplementary material available online at
http://jcs.biologists.org/lookup/suppl/doi:10.1242/jcs.092676/-/DC1

References

Asada, H., Uyemura, K. and Shirao, T. (1994). Actin-binding protein, drebrin, accumulates in submembranous regions in parallel with neuronal differentiation. *J. Neurosci. Res.* **38**, 149-159.

Berryman, M., Franck, Z. and Bretscher, A. (1993). Ezrin is concentrated in the apical microvilli of a wide variety of epithelial cells whereas moesin is found primarily in endothelial cells. *J. Cell Sci.* **105**, 1025-1043.

Bertet, C., Sulak, L. and Lecuit, T. (2004). Myosin-dependent junction remodelling controls planar cell intercalation and axis elongation. *Nature* **429**, 667-671.

Bretscher, A. and Weber, K. (1979). Villin: the major microfilament-associated protein of the intestinal microvillus. *Proc. Natl. Acad. Sci. USA* **76**, 2321-2325.

Bretscher, A. and Weber, K. (1980). Villin is a major protein of the microvillus cytoskeleton which binds both G and F actin in a calcium-dependent manner. *Cell* **20**, 839-847.

Butkevich, E., Hulsmann, S., Wenzel, D., Shirao, T., Duden, R. and Majoul, I. (2004). Drebrin is a novel connexin-43 binding partner that links gap junctions to the submembrane cytoskeleton. *Curr. Biol.* **14**, 650-658.

Chantret, I., Rodolosse, A., Barbat, A., Dussaulx, E., Brot-Laroche, E., Zweibaum, A. and Rousset, M. (1994). Differential expression of sucrase-isomaltase in clones isolated from early and late passages of the cell line Caco-2: evidence for glucose-dependent negative regulation. *J. Cell Sci.* **107**, 213-225.

Drenckhahn, D. and Dermietzel, R. (1988). Organization of the actin filament cytoskeleton in the intestinal brush border: a quantitative and qualitative immunoelectron microscope study. *J. Cell Biol.* **107**, 1037-1048.

Dun, X. P. and Chilton, J. K. (2010). Control of cell shape and plasticity during development and disease by the actin-binding protein Drebrin. *Histol. Histopathol.* **25**, 533-540.

Ezzell, R. M., Chafel, M. M. and Matsudaira, P. T. (1989). Differential localization of villin and fimbrin during development of the mouse visceral endoderm and intestinal epithelium. *Development* **106**, 407-419.

Fath, K. R., Obenauf, S. D. and Burgess, D. R. (1990). Cytoskeletal protein and mRNA accumulation during brush border formation in adult chicken enterocytes. *Development* **109**, 449-459.

Geraldo, S., Khanzada, U. K., Parsons, M., Chilton, J. K. and Gordon-Weeks, P. R. (2008). Targeting of the F-actin-binding protein drebrin by the microtubule plus-tip protein EB3 is required for neuritogenesis. *Nat. Cell Biol.* **10**, 1181-1189.

Gilbert, T., Le Bivic, A., Quaroni, A. and Rodriguez-Boulan, E. (1991). Microtubular organization and its involvement in the biogenetic pathways of plasma membrane proteins in Caco-2 intestinal epithelial cells. *J. Cell Biol.* **113**, 275-288.

Glenney, J. R., Jr, Glenney, P. and Weber, K. (1982). Erythroid spectrin, brain fodrin, and intestinal brush border proteins (TW-260/240) are related molecules containing a common calmodulin-binding subunit bound to a variant cell type-specific subunit. *Proc. Natl. Acad. Sci. USA* **79**, 4002-4005.

Gordon, J. I. and Hermiston, M. L. (1994). Differentiation and self-renewal in the mouse gastrointestinal epithelium. *Curr. Opin. Cell Biol.* **6**, 795-803.

Heintzelman, M. B., Hasson, T. and Mooseker, M. S. (1994). Multiple unconventional myosin domains of the intestinal brush border cytoskeleton. *J. Cell Sci.* **107**, 3535-3543.

Hildebrand, J. D. (2005). Shroom regulates epithelial cell shape via the apical positioning of an actomyosin network. *J. Cell Sci.* **118**, 5191-5203.

Ishikawa, R., Hayashi, K., Shirao, T., Xue, Y., Takagi, T., Sasaki, Y. and Kohama, K. (1994). Drebrin, a development-associated brain protein from rat embryo, causes the dissociation of tropomyosin from actin filaments. *J. Biol. Chem.* **269**, 29928-29933.

Ishikawa, R., Katoh, K., Takahashi, A., Xie, C., Oseki, K., Watanabe, M., Igarashi, M., Nakamura, A. and Kohama, K. (2007). Drebrin attenuates the interaction between actin and myosin-V. *Biochem. Biophs. Res. Commun.* **359**, 398-401.

Jaworski, J., Kapitein, L. C., Gouveia, S. M., Dortland, B. R., Wulf, P. S., Grigoriev, I., Camera, P., Spangler, S. A., Di Stefano, P., Demmers, J. et al. (2009). Dynamic microtubules regulate dendritic spine morphology and synaptic plasticity. *Neuron* **61**, 85-100.

Keon, B. H., Jedrzejewski, P. T., Paul, D. L. and Goodenough, D. A. (2000). Isoform specific expression of the neuronal F-actin binding protein, drebrin, in specialized cells of stomach and kidney epithelia. *J. Cell Sci.* **113**, 325-336.

Le Bivic, A., Bosc-Biern, I. and Reggio, H. (1988). Characterization of a glycoprotein expressed on the basolateral membrane of human intestinal epithelial cells and cultured colonic cell lines. *Eur. J. Cell Biol.* **46**, 113-120.

Lee, C., Scherr, H. M, and Wallingford, J. B. (2007). Shroom family proteins regulate gamma-tubulin distribution and microtubule architecture during epithelial cell shape change. *Development* **134**, 1431-1441.

Lin, C. S., Shen, W., Chen, Z. P., Tu, Y. H. and Matsudaira, P. (1994). Identification of I-plastin, a human fimbrin isoform expressed in intestine and kidney. *Mol. Cell Biol.* **14**, 2457-2467.

Massey-Harroche, D. (2000). Epithelial cell polarity as reflected in enterocytes. *Microsc. Res. Tech.* **49**, 353-362.

Massey-Harroche, D., Delgrossi, M. H., Lane-Guermonprez, L., Arsanto, J. P., Borg, J. P., Billaud, M. and Le Bivic, A. (2007). Evidence for a molecular link between the Tuberous Sclerosis complex and the Crumbs complex. *Hum. Mol. Genet.* **16**, 529-536.

Michel, D., Arsanto, J. P., Massey-Harroche, D., Beclin, C., Wijnholds, J. and Le Bivic, A. (2005). PATJ connects and stabilizes apical and lateral components of tight junctions in human intestinal cells. *J. Cell Sci.* **118**, 4049-4057.

Mizui, T., Kojima, N., Yamazaki, H., Katayama, M., Hanamura, K. and Shirao, T. (2009). Drebrin E is involved in the regulation of axonal growth through actin-myosin interactions. *J. Neurochem.* **109**, 611-622.

Mooseker, M. S. (1985). Organization, chemistry, and assembly of the cytoskeletal apparatus of the intestinal brush border. *Annu. Rev. Cell Biol.* **1**, 209-241.

Mooseker, M. S. and Tilney, L. G. (1975). Organization of an actin filament-membrane complex. Filament polarity and membrane attachment in the microvilli of intestinal epithelial cells. *J. Cell Biol.* **67**, 725-743.

Nakajima, H. and Tanoue, T. (2010). Epithelial cell shape is regulated by Lulu proteins via myosin-II. *J. Cell Sci.* **123**, 555-566.

Otani, T., Ichii, T., Aono, S. and Takeichi, M. (2006). Cdc42 GEF Tuba regulates the junctional configuration of simple epithelial cells. *J. Cell Biol.* **175**, 135-146.

Pearl, M., Fishkind, D., Mooseker, M., Keene, D. and Keller, T., 3rd. (1984). Studies on the spectrin-like protein from the intestinal brush border, TW 260/240, and characterization of its interaction with the cytoskeleton and actin. *J. Cell Biol.* **98**, 66-78.

Peterson, M. D. and Mooseker, M. S. (1992). Characterization of the enterocyte-like brush border cytoskeleton of the C2BBe clones of the human intestinal cell line, Caco-2. *J. Cell Sci.* **102**, 581-600.

Peterson, M. D. and Mooseker, M. S. (1993). An in vitro model for the analysis of intestinal brush border assembly. I. Ultrastructural analysis of cell contact-induced brush border assembly in Caco-2BBe cells. *J. Cell Sci.* **105**, 445-460.

Peterson, M. D., Bement, W. M. and Mooseker, M. S. (1993). An in vitro model for the analysis of intestinal brush border assembly. II. Changes in expression and localization of brush border proteins during cell contact-induced brush border assembly in Caco-2BBe cells. *J. Cell Sci.* **105**, 461-472.

Rodriguez-Boulan, E. and Nelson, W. J. (1989). Morphogenesis of the polarized epithelial cell phenotype. *Science* **245**, 718-725.

Rodriguez-Boulan, E., Salas, P. J., Sargiacomo, M., Lisanti, M., Le Bivic, A., Sambuy, Y., Vega-Salas, D. and Graeve, L. (1989). Methods to estimate the polarized distribution of surface antigens in cultured epithelial cells. *Methods Cell Biol.* **32**, 37-56.

Rogers, S. L., Wiedemann, U., Hacker, U., Turck, C. and Vale, R. D. (2004). Drosophila RhoGEF2 associates with microtubule plus ends in an EB1-dependent manner. *Curr. Biol.* **14**, 1827-1833.

Rolo, A., Skoglund, P. and Keller, R. (2009). Morphogenetic movements driving neural tube closure in Xenopus require myosin IIB. *Dev. Biol.* **327**, 327-338.

Rousset, M. (1986). The human colon carcinoma cell lines HT-29 and Caco-2: two in vitro models for the study of intestinal differentiation. *Biochimie* **68**, 1035-1040.

Saaf, A. M., Halbleib, J. M., Chen, X., Yuen, S. T., Leung, S. Y., Nelson, W. J. and Brown, P. O. (2007). Parallels between global transcriptional programs of polarizing Caco-2 intestinal epithelial cells in vitro and gene expression programs in normal colon and colon cancer. *Mol. Biol. Cell* **18**, 4245-4260.

Saotome, I., Curto, M. and McClatchey, A. I. (2004). Ezrin is essential for epithelial organization and villus morphogenesis in the developing intestine. *Dev. Cell* **6**, 855-864.

Shirao, T. and Obata, K. (1985). Two acidic proteins associated with brain development in chick embryo. *J. Neurochem.* **44**, 1210-1216.

Stepanova, T., Slemmer, J., Hoogenraad, C. C., Lansbergen, G., Dortland, B., De Zeeuw, C. L., Grosveld, F., van Cappellen, G., Akhmanova, A. and Galjart, N. (2003). Visualization of microtubule growth in cultured neurons via the use of EB3-GFP. *J. Neurosci.* **23**, 2655-2664.

Takahashi, H., Sekino, Y., Tanaka, S., Mizui, T., Kishi, S. and Shirao, T. (2003). Drebrin-dependent actin clustering in dendritic filopodia governs synaptic targeting of postsynaptic density-95 and dendritic spine morphogenesis. *J. Neurosci.* **23**, 6586-6595.

Tokuyasu, K. T. (1978). A study of positive staining of ultrathin frozen sections. *J. Ultrastruct. Res.* **63**, 287-307.

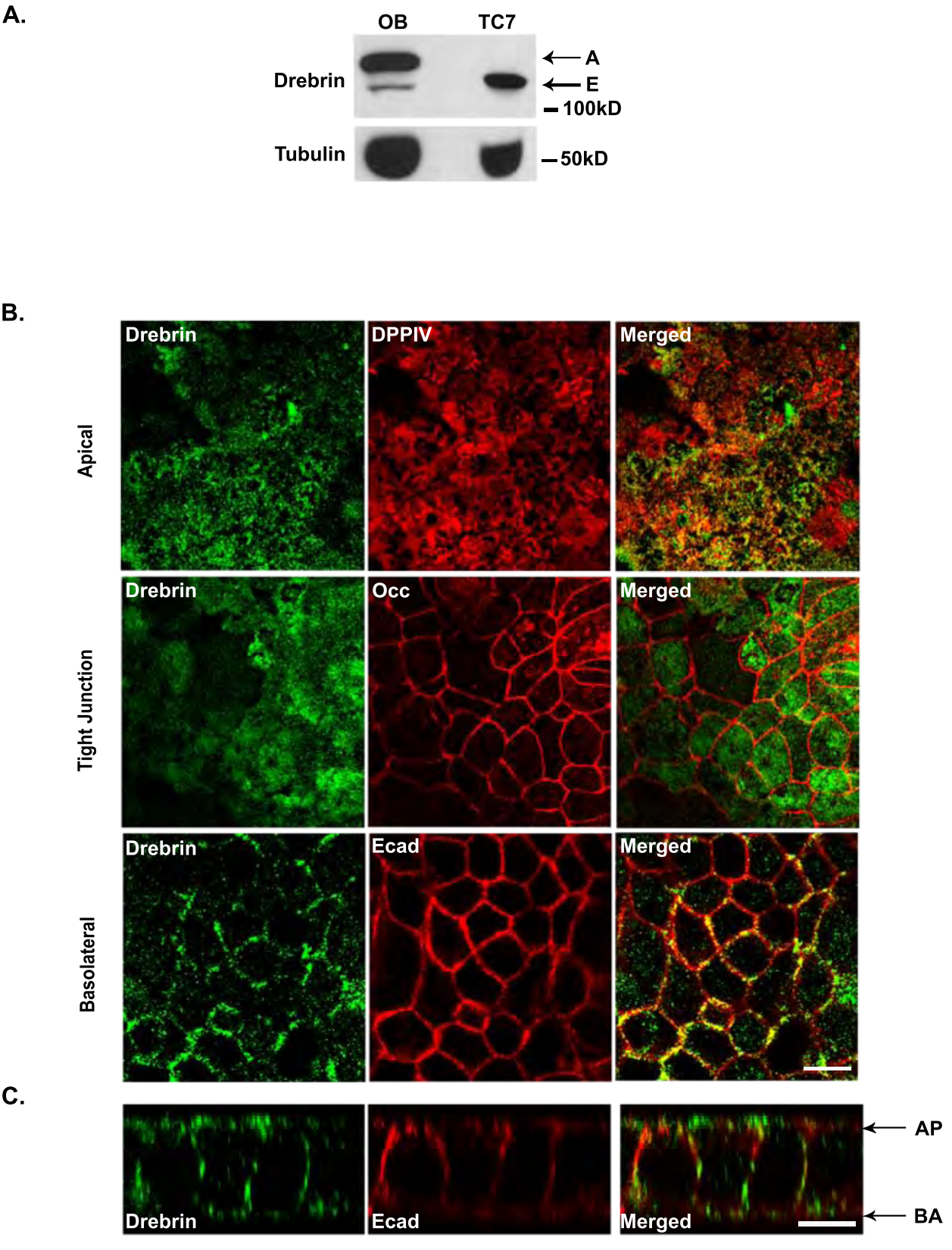
A.
OB
TC7
Drebrin
A
E
100kD
Tubulin
50kD
B.
Drebrin
DPPIV
Merged
Apical
Drebrin
Occ
Merged
Tight Junction
Drebrin
Ecad
Merged
Basolateral
C.
Drebrin
Ecad
Merged
AP
BA

A.

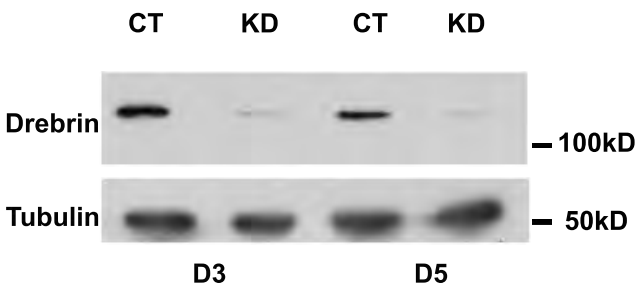
CT
KD
CT
KD
Drebrin
100kD
Tubulin
50kD
D3
D5

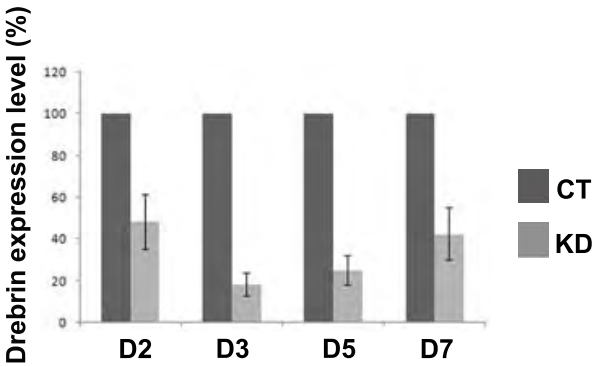
Drebrin expression level (%)
120
100
80
60
40
20
0
D2
D3
D5
D7
CT
KD

B.

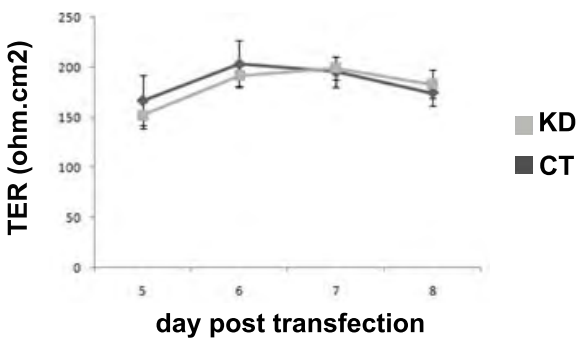
TER (ohm.cm2)
250
200
150
100
50
0
5
6
7
8
day post transfection
KD
CT

C.

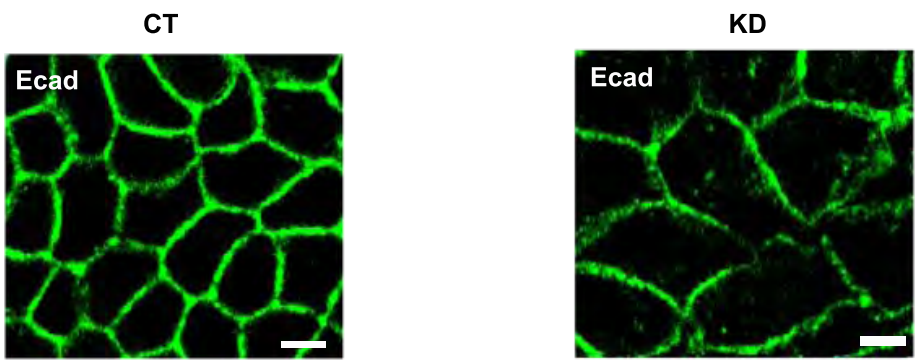
CT
KD
Ecad
Ecad

D.

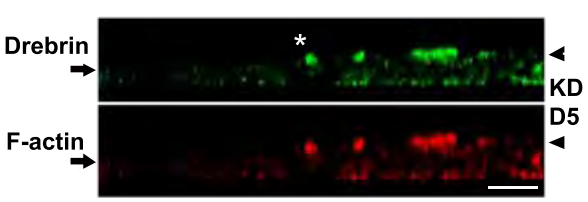
Drebrin
*
KD
D5
F-actin

A

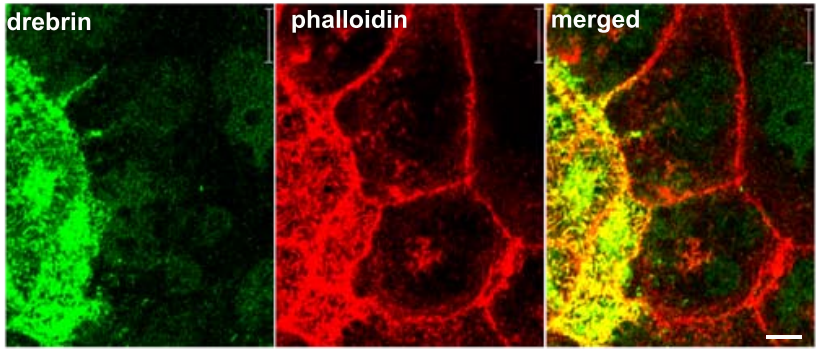

B

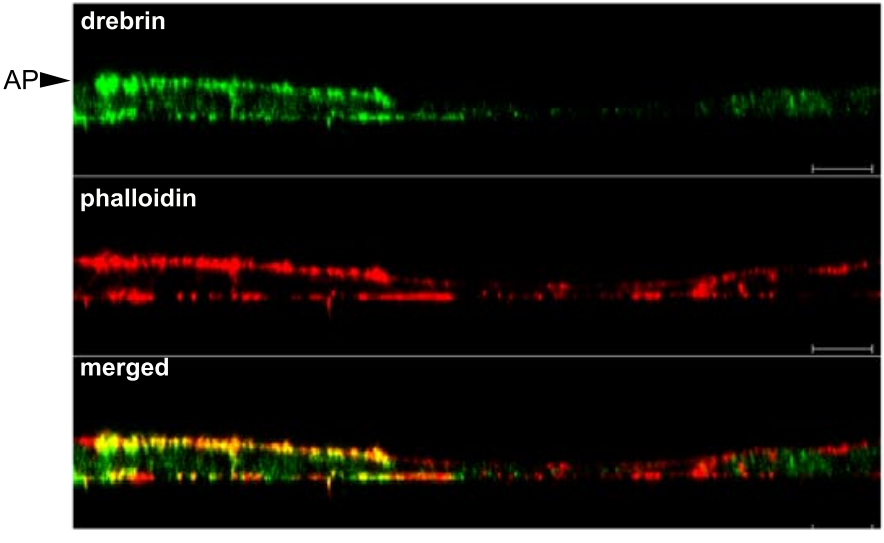

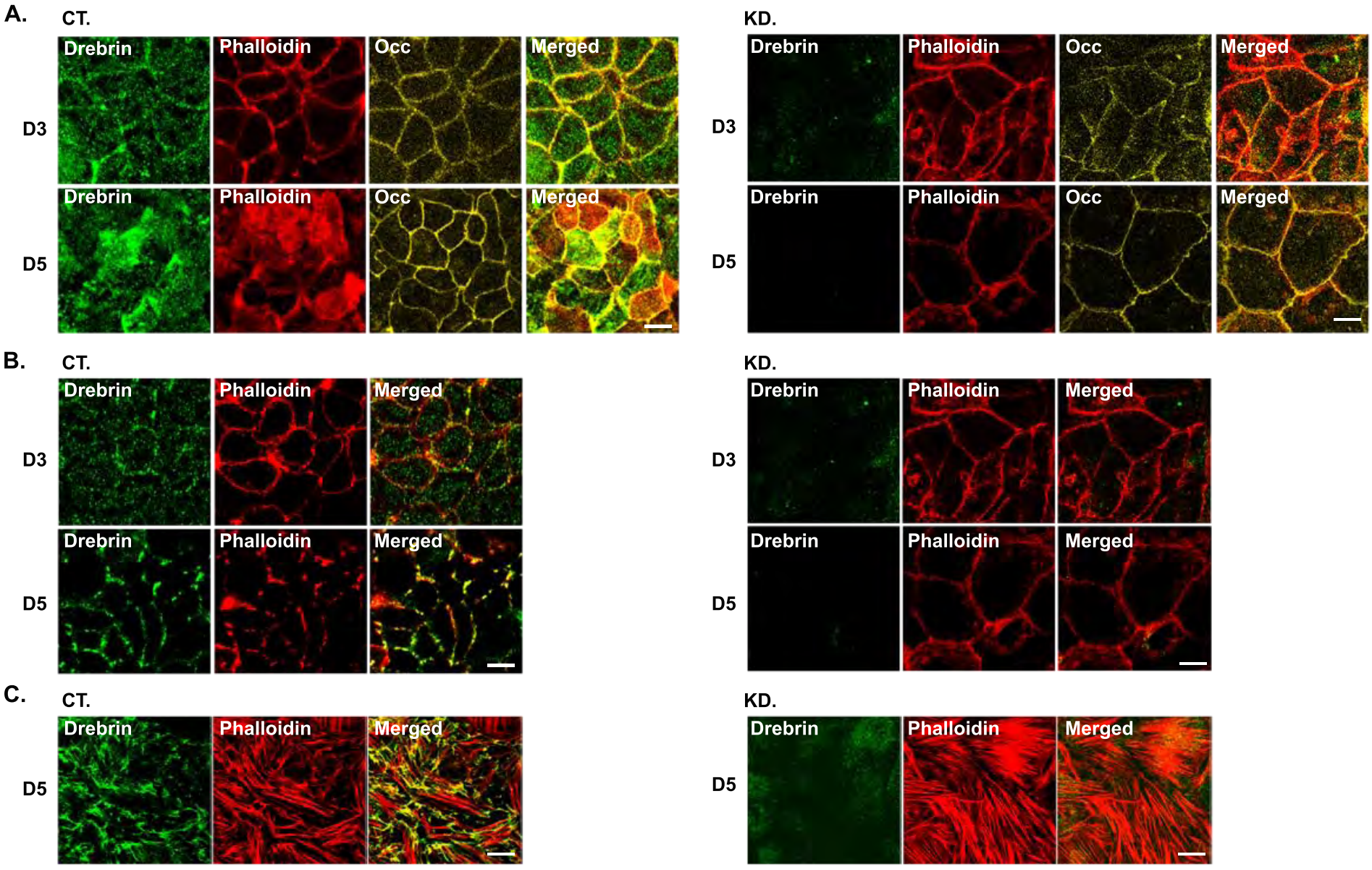
A.
CT.
KD.
Drebrin
Phalloidin
Occ
Merged
D3
D5
B.
C.

A.

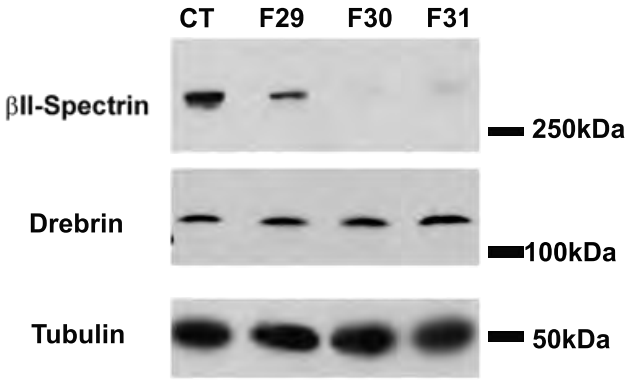
CT
F29
F30
F31
βII-Spectrin
250kDa
Drebrin
100kDa
Tubulin
50kDa

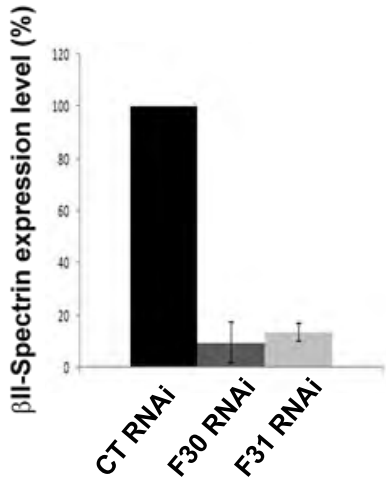
βII-Spectrin expression level (%)
120
100
80
60
40
20
0
CT RNAi
F30 RNAi
F31 RNAi

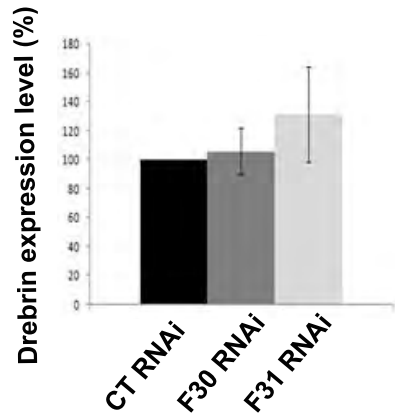
Drebrin expression level (%)
180
160
140
120
100
80
60
40
20
0
CT RNAi
F30 RNAi
F31 RNAi

B.

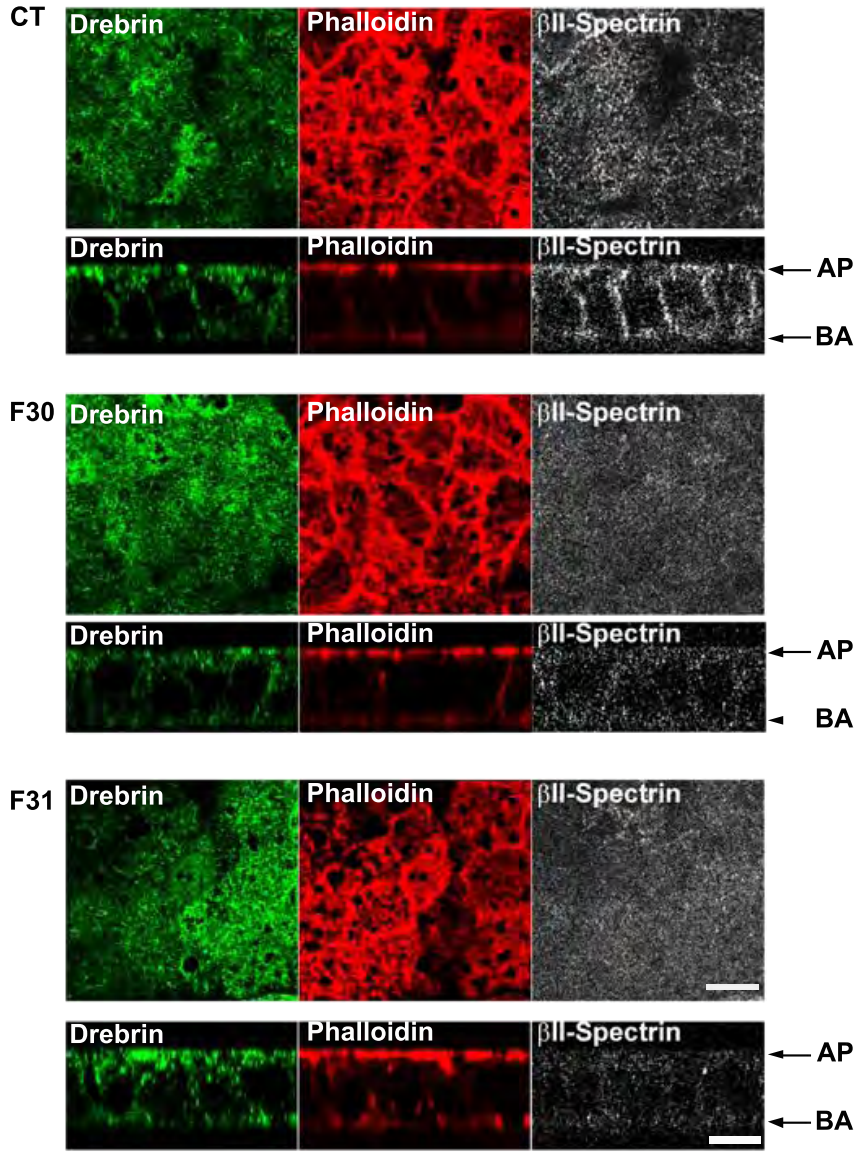
CT
Drebrin
Phalloidin
βII-Spectrin
AP
BA
F30
Drebrin
Phalloidin
βII-Spectrin
AP
BA
F31
Drebrin
Phalloidin
βII-Spectrin
AP
BA

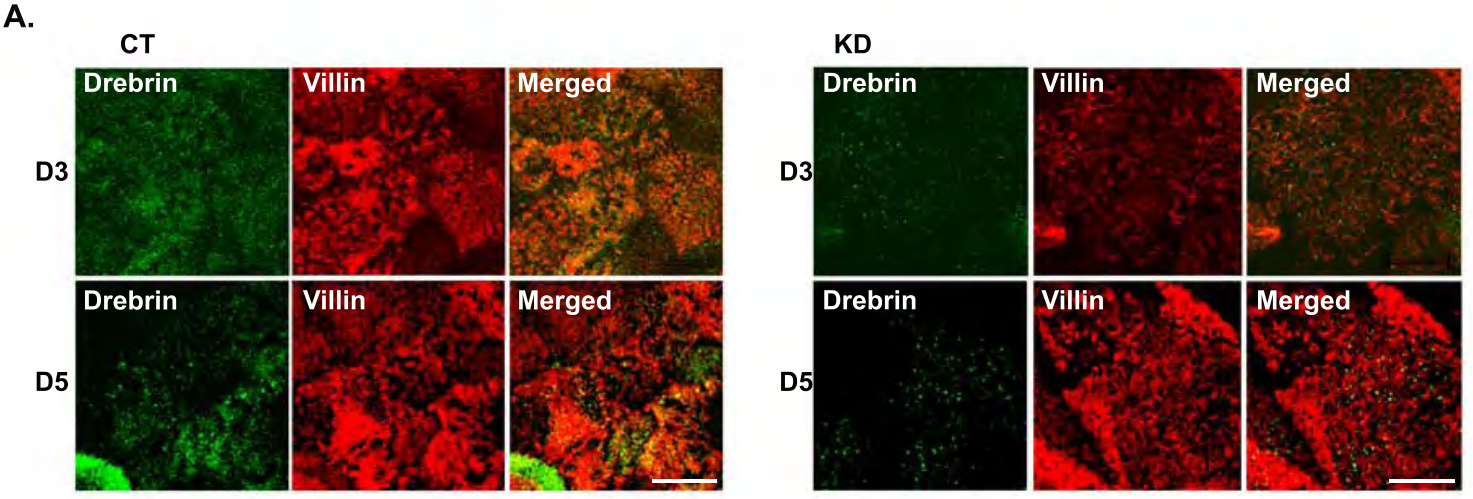
A.
CT
KD
Drebrin
Villin
Merged
D3
D5

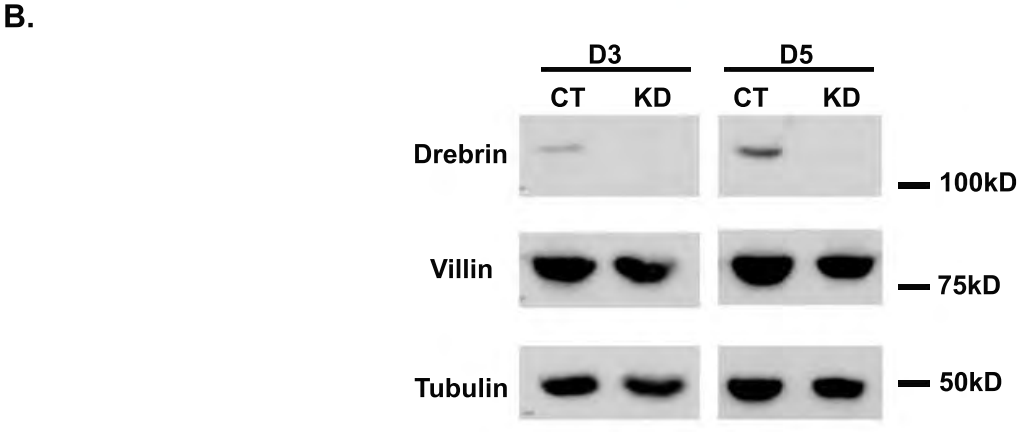
B.
D3
D5
CT
KD
Drebrin
Villin
Tubulin
100kD
75kD
50kD

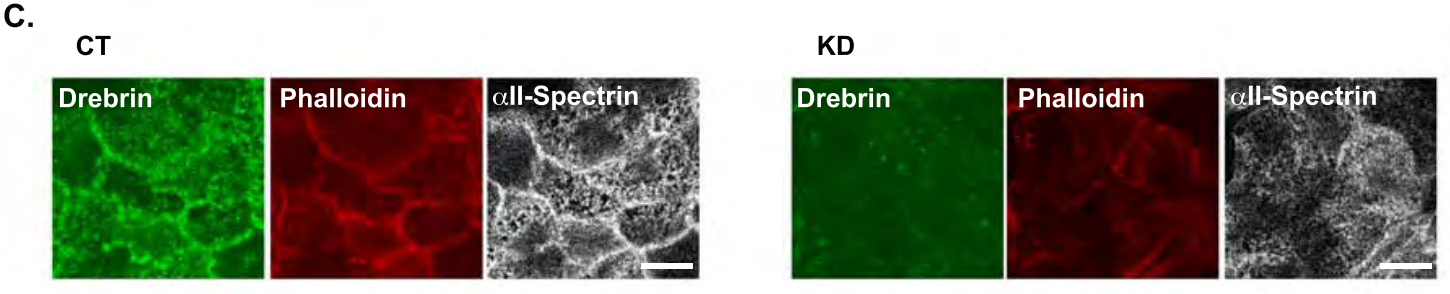
C.
CT
KD
Drebrin
Phalloidin
αII-Spectrin